

## 附件 2

项目名称	基于滑模观测器和电容电压变化率的 MMC 关键元件故障诊断方法研究
项目类别	<input type="checkbox"/> C 类 <input checked="" type="checkbox"/> D 类
产业领域	<input type="checkbox"/> 信息 <input type="checkbox"/> 环保 <input type="checkbox"/> 健康 <input type="checkbox"/> 旅游 <input type="checkbox"/> 时尚 <input type="checkbox"/> 金融 <input type="checkbox"/> 高端装备制造 <input type="checkbox"/> 文化创意 <input type="checkbox"/> 海洋经济 <input type="checkbox"/> 生物技术 <input checked="" type="checkbox"/> 新能源 <input type="checkbox"/> 新材料 <input type="checkbox"/> 其他
所在平台	<input type="checkbox"/> 省级留学人员创业园 : _____ <input type="checkbox"/> 省重点企业研究院: _____ <input type="checkbox"/> 省级产业集聚区: _____ <input checked="" type="checkbox"/> 其他
是否回国来浙 从事博士后 研究工作	<input type="checkbox"/> 是, 海外博士授予学校: _____ 回国时间: _____ 博士后编号: _____
	<input checked="" type="checkbox"/> 否

# 浙江省“钱江人才计划”C、D 类 项目申请表

姓 名 \_\_\_\_\_ 邵帅  
单 位 \_\_\_\_\_ 浙江大学  
部门(地区) \_\_\_\_\_ 电气工程学院

浙江省人力资源和社会保障厅

## 填 表 说 明

1、产业领域：请在以下相应产业领域栏目打“√”：信息、健康、环保、旅游、时尚、金融、高端装备制造、文化创意、海洋经济、生物技术、新能源、新材料；不属上述产业领域的，请在“其他”栏打“√”。

2. 所在平台：若项目属省级留学人员创业园、省重点企业研究院、省级产业集聚区的，请在相应栏打“√”，并填写相应名称。不属于上述内容的，请在“其他”栏打“√”。

3、是否回国来浙从事博士后研究工作：在“是”或“否”前打“√”，若是，填写相应栏目。

4、表内各栏目填写内容的起讫时间均为最近 5 年，例如，2016 年申请的，各栏日起讫时间为 2011 年 1 月至今。



<p>从事专业 工作情况</p>	<p>(概述本人的专业研究领域、方向和主要业绩)</p> <p>申请人从事的专业为电力电子技术，依靠功率电力电子器件实现电能的高效率变换与控制，是一门融合了电气工程、电子科学与技术、控制理论三大学科的交叉学科。电力电子技术是太阳能、风能等新能源并网，电网智能化，高压直流输电，电动汽车，高速铁路电机牵引，以及多电飞机等高新领域的核心技术。</p> <p>申请人研究方向是柔性直流输电技术，作为新一代的直流输电技术，在大规模风电场并网、交流系统互联、城市配电网的增容改进等应用场合要较强最具潜力的技术。一般的柔性直流输电系统由两个模块化多电平变换器(Modular Multilevel Converter, MMC)背靠背构成。一个 MMC 可包含上千个子模块，这些子模块若发生故障，将损坏其他元器件，可能造成系统瘫痪，造成较大的经济损失。申请人自 2011 年起研究 MMC 的故障诊断工作，提出两种基于滑模观测器的诊断方法，在 MMC 发生故障后，能在 20 毫秒左右定位故障，有利于提高柔性直流输电系统的可靠性，发表电力电子领域国际顶级期刊 <i>IEEE Trans. Power Electron.</i> (影响因子 6.008) 论文 2 篇，其中一篇他引 33 次。</p>
----------------------	---



## 二、五年来主要成果

1、参与过的主要项目				
项目名称	起止时间	项目性质和来源	经费总额	参与人数、本人排名和任务
敏感负荷电压暂降控制器的研制	2015.10-2016.09	江苏金智科技股份有限公司合作项	60万	5、3、系统设计和调试

2、代表性论文、著作（不超过20项）				
论文、著作名称	发表/出版时间	发表/出版载体	论文索引情况	本人排名
Fault Detection for Modular Multilevel Converters Based on Sliding Mode Observer	2013	<i>IEEE Trans. Power Electron.</i>	33	1
Robustness Analysis and Experimental Validation of a Fault Detection and Isolation Method for the Modular Multilevel Converter	2016	<i>IEEE Trans. Power Electron.</i>	0	1
Detection and isolation of multiple faults in a modular multilevel converter based on a sliding mode observer	2014	<i>IEEE ECCE 2014</i>	0	1
Open-circuit fault detection and isolation for modular multilevel converter based on sliding mode observer	2013	<i>EPE 2013</i>	0	1

3、专利					
专利名称	专利类别	批准时间	授权国家	是否投产	本人排名

4、产品（如有产品，说明目前的产业化程度）

5、其他（包括获得的重要奖项、在国际学术会议做重要报告等情况）

### 三、项目可行性说明

#### 1、立项背景（说明项目意义、国内外研究现状和发展趋势）。

最初的柔性直流输电系统(Voltage Sourced Converter based High Voltage DC Transmission, VSC-HVDC)普遍采用两电平或者三电平中性点钳位型(Neutral Point Clamped, NPC)变换器。单个电力电子开关器件耐压能力有限，为应对 HVDC 中的高电压，需要将多个开关器件串联起来使用。开关器件串联存在两个问题，一是均压，即如何在开关瞬态及关断状态下，使电压平均地分配在各个串联的器件之上；二是开路故障，即单个器件的开路故障将使所有与之串联的器件失效。解决这两个问题难度较大，目前只有 ABB 公司克服这些技术障碍，将基于两电平和三电平的 VSC-HVDC 成功商业化。除了上述问题，两电平或三电平的变换器的输出电能质量差，需要采用较大的滤波器来滤除谐波；而且变换器损耗大，效率最高只有 98% 左右[1]。

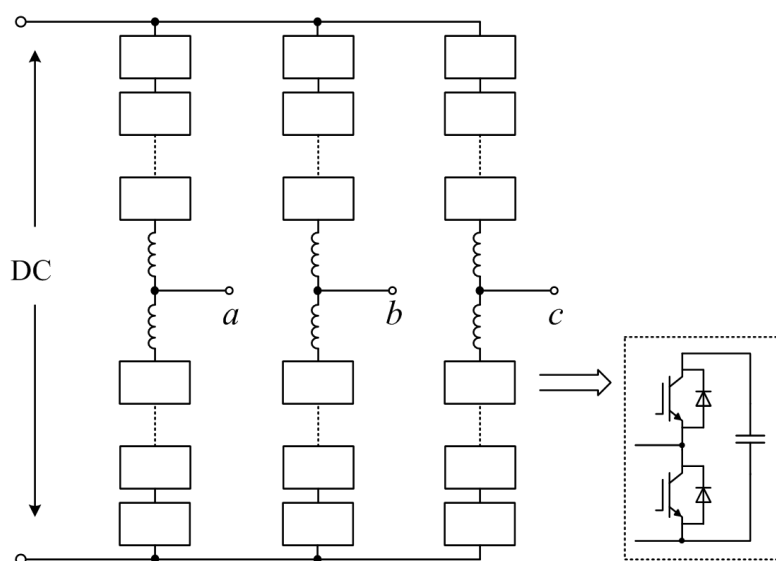


图 1. MMC 拓扑图.

2001 年德国的 R. Marquardt 教授提出了模块化多电平变换器(Modular Multilevel Converter)，拓扑如图 1 所示，具有以下优点[2]：

- 由大量相同模块（半桥或全桥结构）级联而成，可适应不同等级电压，且降低了制造成本；
- 输出交流电压为多电平阶梯波，电能质量高，大大减小了滤波器；

- 易于实现冗余，发生故障后，只需将故障子模块旁路并插入冗余子模块即可；
- 效率高，最高效率可达到 99.5%。

由于以上优点，加之具有公共的直流母线，MMC 极为适合高压直流输电场合，迅速被工业界采用。2010 年 11 月，由西门子承建的世界第一个基于 MMC 的柔性直流输电系统 Trans Bay Cable 便已投入使用，展现了良好的技术特性 [3]。ABB 和 Alstom 也相继开展研究，推出了类似产品。目前，MMC 取代两电平和三电平变换器，成为柔性直流输电的主流拓扑。国内对柔性直流输电技术的研究起步于 2003 年，取得了快速发展，目前已有上海南汇示范工程（20MW/±30kV，2011 年），南澳多端口（200MW/±160kV，2013 年），舟山多端口（400WM/±200kV，2014 年），厦门示范工程（1000MW/±320kV，2015 年）等工程投运[4]。

MMC 由大量模块级联而成，含有数目众多的电力电子器件和电容，例如 Trans Bay Cable 项目中，就包含超过 2400 个 IGBT 和 1200 电容器[3]。而根据 S. Yang 等学者的工业调查结果，电力电子器件和电容是变换器中故障率最高的元器件[5]。因而，MMC 元件的故障率要天然地高于其他变换器。单个元件的故障会降低输出电能质量，并产生局部高电压大电流，波及其他元器件（即引起二次故障），进而可能造成整个 HVDC 系统瘫痪。纵观国内外投入使用的 MMC 柔性直流输电系统，功率范围一般在数百到数千兆瓦，未来更有可能再提高一个数量级。系统一旦因故障而瘫痪，将造成大面积停电。现代工业高度依赖电力，停电将造成巨大的国民经济损失，例如 2013 年 5 月 21 日，泰国南部多地停电 3 小时左右，就造成了约合 3.5 亿美元的经济损失[6]。如何提高 MMC-HVDC 系统的可靠性，保证其不间断运行成为了一个极为重要而富有挑战性的研究课题，这其中很重要的分支就是 MMC 关键元件 IGBT 和电容器的故障诊断。

本项目针对 MMC 中功率器件 IGBT 和电容器可能出现的故障:IGBT 开路故障、短路故障和电容老化，提出一整套简单可靠的解决方案。这些方案能准确快速地定位故障。被定位的故障子模块将被旁路，并插入冗余子模块，保证 MMC 系统的不间断运行。下面先对已有故障诊断方法进行归纳总结。

### **IGBT 的故障诊断**

电力电子器件的故障分为开路故障和短路故障。IGBT 开路故障是指器件一直处

于断开状态，不受门极信号控制，产生原因有模块内部焊接层、绑定线疲劳断裂，或者门极驱动故障[7]。IGBT 短路故障则是指器件处于导通状态，不受控制，器件过流或者过压皆可能导致短路故障。对于电力电子器件的故障诊断，国内外学者已经做过大量工作。总结起来，根据采用的手段，功率器件的故障诊断方法可分为两类，一是硬件方法，二是软件方法。硬件方法添加额外的传感器来检测电压、电流和温度等信号，并通过逻辑电路处理这些信号，当它们超过一定的阈值，即认为电路发生了故障。下面分析各类 IGBT 故障诊断硬件方法的优缺点：

1)  $V_{ce}$  退保和检测。IGBT 的集电极-发射极压降  $V_{ce}$  与流经 IGBT 的电流在一定范围内存在线性关系，当 IGBT 因短路出现过流时， $V_{ce}$  将显著高于正常值，利用这个特性可判断 IGBT 是否有短路故障[8]。这种方法简单有效，能在 IGBT 过流时及时关断器件，使其免受损坏，很多门极驱动芯片都集成了此项功能。但是该方法只在 IGBT 损坏前有效，且无法检测过压导致的短路故障。

2) IGBT 电流  $i_c$  检测。通过检测流经 IGBT 的电流  $i_c$  来判断故障，传感器可采用霍尔元件、罗氏线圈 (Rogowski Coil) 或者高可靠电阻，通过一个逻辑电路产生故障信号[9]。这种方法可以分辨开路或者短路故障。然而在 MMC-HVDC 中，流经 IGBT 的电流可达上千安培，采集如此大电流的霍尔元件或罗氏线圈成本较高；电阻则损耗大，不适合于大电流应用场合。

3) 镜像电流检测。利用镜像电路来获取 IGBT 的电流，镜像电路由一个小型 IGBT 和电阻串联而成，与主 IGBT 并联。流经主 IGBT 的电流可由镜像电路中电阻的压降算得。根据该压降及门极信号，可判断 IGBT 的开路或者短路故障[10]。此方法将增大主功率电路的复杂度，且成本较高 (需要一个额外的 IGBT)。

4)  $di_c/dt$  检测。美国田纳西州立大学的 L. Tolbert 等学者把 IGBT 电流斜率  $di_c/dt$  作为反馈以提高 IGBT 的开关速率， $di_c/dt$  也可以来检测过流故障[11]。该方法速度快，但是电路很复杂，其本身就有发生故障的可能性。

4) 门极信号检测。M. A. R-Blanco 等学者通过检测门极电压上升沿米勒平台时间，来判断 IGBT 器件是否有开路或短路故障，检测时间只需要  $3 \mu s$  [12]。L. Chen 等学者通过检测 IGBT 门极的充放电电流来诊断开路或短路故障[13]。这类方法速度快，成本低，但是只在开关瞬态起作用，对于在导通状态时发生的故障，要到下

一个开关周期方能检测，不适用于开关频率较低的情况。

硬件诊断法虽然可靠性高，检测速度快，但是额外的传感器和电路增加了体积和成本，而且这些传感器和电路本身也有发生故障的可能性。软件诊断法则另辟蹊径，利用已有的信号如用于反馈控制的电压、电流及门极驱动信号，来诊断故障。这些信号具有一定相关性，且这种相关性在正常和故障情况下不一致，利用此差异可将故障诊断出来。变换器信号的相关性可根据变换器的解析模型获得。

两电平逆变器输出电流可用于检测 IGBT 开路故障，包括平均电流 Park 矢量法、三相电流平均值法、基于傅里叶变换的归一化方法等，哈尔滨工业大学的于咏副教授对电流检测法进行了很好的总结[14]。这一类方法不适合 MMC 等多电平变换器，因为无法定位故障的具体位置。另外，变换器的输出电压也能用于故障诊断。Meynard 等学者从飞跨电容钳位型 (Flying Capacitor Clamped) 多电平变换器的输出电压中提取开关频率分量  $\bar{v}_s$ ：正常情况下，该分量幅值  $|\bar{v}_s|$  很小；出现故障时， $|\bar{v}_s|$  显著变大， $\bar{v}_s$  的角度可用于指示故障的具体位置[15]。A. Yazdani 等学者则在时域内分析输出电压，通过比较实际与理想的输出电压找寻故障[16]。这类方法能够用于各类多电平变换器，但是当电平数目变大时，故障诊断的正确率会急剧下降：故障引起输出电压的变化将非常之小，无法分辨是噪声还是故障，此外这些方法在多个故障并发时无法有效诊断。L. Tolbert 等学者还将人工智能应用于多电平变换器的故障检测，但是诊断准确率在有些情况下只有 76%，易发生误诊断[17]。申请人在诺丁汉大学攻读博士期间从事 MMC 子模块 IGBT 的开路故障诊断，基于滑模观测器 (Sliding Mode Observer, SMO)，采用猜想-验证的思想，能在 20 毫秒左右定位开路故障[18, 19]，但是该方法在多个开路故障并发时亦无法有效诊断，因为有过多的故障位置需要猜测，导致计算量过大。

### 电容的故障检测

常用于直流母线的电容有三种：铝电解电容、金属薄膜电容和多层瓷片电容[20]。相较于其他两类电容，金属薄膜电容在可靠性、纹波电流承受能力、寄生电阻和成本等方面达到了一个较好的均衡，实际的 MMC-HVDC 工程项目一般采用这种电容作为子模块电容[20]。然而金属薄膜电容仍会随时间而老化，老化的机理一是金属

化膜自愈，二是金属化膜腐蚀[20, 21]。一般，当电容量的下降超过 5%~10%时（因不同厂商而异），金属薄膜电容性能急剧恶化，通常把电容量损失达到初始值的 5%~10%作为电容寿命终结的标志[20, 21]。

为了提高电容的寿命，一方面可以采用更加先进的制造工艺。根据前期调研，国内 MMC-HVDC 供应商为了提高工程的可靠性，电容一般从国外 Vishay 等公司进口，确保其使用寿命在 20~30 年。显然，先进的工艺的意味着高成本。另一方面，也可以通过软件方式监测电容的健康状况，提高工程的可靠性。

国内外学者一般采用  $C = (\int i_c dt) / \Delta v_c$  来估计电容量，其中  $i_c$  是流经电容的电流， $\Delta v_c$  是电容电压纹波[20, 22, 23]。A. Wechsler 等学者利用此方法在线估计航天器上电机驱动的直流母线电容值，使其具有容错功能，但是精确度低，最大误差达 4.3%[22]。Y.-J. Jo 等学者添加低频滤波器，并借助递归最小二乘法在线估计 MMC 子模块电容量，将估计误差减小到了 1.3%[23]。但是该方法算法复杂，计算量大，实施难度较大。K.-W. Lee 等学者用离线方式估计电容量以调高准确率：在变换器空闲时，添加一个低频、固定占空比的 PWM 信号，增大  $\Delta v_c$  的值，减小因噪声造成的误差[24]。然而，离线方式不适合 MMC 子模块电容量的估计—MMC-HVDC 需要不间断工作。

从国内外研究的最新进展可以看出，MMC 的子模块 IGBT 的故障检测虽然已有多种方法，但是均存在着不足：硬件诊断方法中，1) 退保和检测简单可靠、应用广泛，但只在 IGBT 损坏前有效，且无法检测过压导致的短路故障；2)  $i_c$  检测、镜像电流法需要测量流经 IGBT 的大电流，额外的传感器成本高，增加了主功率电路的复杂度；3)  $di/dt$  检测电路过于复杂，其本身就有可能发生故障；4) 门极信号检测不适合于低频电路如 MMC。软件诊断方法中，传统的基于分析输出电流或输出电压的各类方法不适合于模块数众多的 MMC，申请人提出的基于滑模观测器的诊断法，能快速准确地（20ms）诊断单个开路故障，但是对多个故障并发时仍存在问题。

为此，申请人针对 MMC 中 IGBT 的开路和短路故障，以及电容的老化，提出一套可靠、快速、简单的诊断方法。对于子模块 IGBT 的开路故障以及电容的健康状况监测，提出基于滑模观测器的诊断方法：利用已有的子模块电流、电容电压和门极信号，给每个子模块建立观测器，实时估计电容电压和电容量，通过比较估计

与实际的电容电压，判断是否有开路故障；通过电容量的减少程度，判断电容的健康状况。

MMC 子模块由半桥（或 H 桥）和一个电容组成（见图 1），IGBT 短路将造成子模块桥臂直通，电容急剧放电，电容电压迅速下降，下降速度远远大于因功率交换引起的波动。本项目利用 MMC 这一特有现象，提出一种基于判断电容电压变化率的 IGBT 短路故障诊断电路。该电路结构简单(只需要无源元件、比较器和逻辑门)，通过检测电容电压的变化速率，并结合门极信号，诊断 IGBT 的短路故障。

IGBT 的开路或短路故障被定位后，故障子模块将被切除，冗余子模块被插入，使 MMC 不间断运行；子模块电容的老化状况则可用来微调各模块的使用率：电容老化严重的模块少使用一点，电容较健康的模块多使用一点，最终提高 MMC 电容的整体寿命。本项目的开展，能较大幅度的提高 MMC 的可靠性，为 MMC 柔性直流输电系统的不间断运行保驾护航，为柔性高压输电系统的推广、及未来高压直流大电网的建设做出贡献。

### 参考文献

- [1] M. Barnes, and A. Beddard, "Voltage Source Converter HVDC Links – The State of the Art and Issues Going Forward," *Energy Procedia*, vol. 24, pp. 108-122, 2012.
- [2] M. A. Perez, S. Bernet, J. Rodriguez, S. Kouro, and R. Lizana, "Circuit Topologies, Modeling, Control Schemes, and Applications of Modular Multilevel Converters," *Power Electronics, IEEE Transactions on*, vol. 30, no. 1, pp. 4-17, 2015.
- [3] B. Gemmel, J. Dorn, D. Retzmann, and D. Soerangr, "Prospects of multilevel VSC technologies for power transmission." pp. 1-16.
- [4] 李岩, 罗雨, 许树楷, 周月宾, 袁志昌, 柔性直流输电技术: 应用、进步与期望, 南方电网技术, no. 01, pp. 7-13, 2015.
- [5] Y. Shaoyong, A. Bryant, P. Mawby, X. Dawei, L. Ran, and P. Tavner, "An Industry-Based Survey of Reliability in Power Electronic Converters," *Industry Applications, IEEE Transactions on*, vol. 47, no. 3, pp. 1441-1451, 2011.
- [6] 常天童, 泰国南部大范围停电造成巨大经济损失, 新华网 [http://news.xinhuanet.com/2013-05/22/c\\_115870388.htm](http://news.xinhuanet.com/2013-05/22/c_115870388.htm), 2013.5.22.
- [7] S. Shao, "The application of Sliding Mode Observers to Fault Detection and Isolation for Multilevel Converters," PhD, University of Nottingham, 2015.
- [8] R. S. Chokhawala, J. Catt, and L. Kiraly, "A discussion on IGBT short-circuit behavior and fault protection schemes," *Industry Applications, IEEE Transactions on*, vol. 31, no. 2, pp. 256-263, 1995.
- [9] 刘海红, 杨媛, 刘海锋. 大功率 IGBT 驱动保护方法研究进展综述. 电子设计工程, no. 07, pp. 104-106+110, 2015.



- [10] L. Bin, and S. K. Sharma, "A Literature Review of IGBT Fault Diagnostic and Protection Methods for Power Inverters," *Industry Applications, IEEE Transactions on*, vol. 45, no. 5, pp. 1770-1777, 2009.
- [11] W. Zhiqiang, S. Xiaojie, L. M. Tolbert, W. Fei, and B. J. Blalock, "A di/dt Feedback-Based Active Gate Driver for Smart Switching and Fast Overcurrent Protection of IGBT Modules," *Power Electronics, IEEE Transactions on*, vol. 29, no. 7, pp. 3720-3732, 2014.
- [12] Rodri, x, M. A. guez-Blanco, S. Claudio, x, A. nchez, D. Theilliol, V. Vela, x, L. G s, T. Sibaja, x, P. n, Herna, x, G. ndez, x, L. lez, and J. Aguayo-Alquicira, "A Failure-Detection Strategy for IGBT Based on Gate-Voltage Behavior Applied to a Motor Drive System," *Industrial Electronics, IEEE Transactions on*, vol. 58, no. 5, pp. 1625-1633, 2011.
- [13] C. Lihua, F. Z. Peng, and C. Dong, "A smart gate drive with self-diagnosis for power MOSFETs and IGBTs." pp. 1602-1607.
- [14] 于泳, 蒋生成, 杨荣峰, 王高林, 徐殿国. 变频器 IGBT 开路故障诊断方法. *中国电机工程学报*, vol. 31, no. 9, pp. 30-35, 2011.
- [15] F. Richardeau, P. Baudesson, and T. A. Meynard, "Failures-tolerance and remedial strategies of a PWM multicell inverter," *Power Electronics, IEEE Transactions on*, vol. 17, no. 6, pp. 905-912, 2002.
- [16] A. Yazdani, H. Sepahvand, M. L. Crow, and M. Ferdowsi, "Fault Detection and Mitigation in Multilevel Converter STATCOMs," *Industrial Electronics, IEEE Transactions on*, vol. 58, no. 4, pp. 1307-1315, 2011.
- [17] S. Khomfoi, and L. M. Tolbert, "Fault Diagnosis and Reconfiguration for Multilevel Inverter Drive Using AI-Based Techniques," *Industrial Electronics, IEEE Transactions on*, vol. 54, no. 6, pp. 2954-2968, 2007.
- [18] S. Shao, A. J. Watson, J. C. Clare, and P. W. Wheeler, "Robustness Analysis and Experimental Validation of a Fault Detection and Isolation Method for the Modular Multilevel Converter," *Power Electronics, IEEE Transactions on*, vol. 31, no. 5, pp. 3794-3805, 2016.
- [19] S. Shuai, P. W. Wheeler, J. C. Clare, and A. J. Watson, "Fault Detection for Modular Multilevel Converters Based on Sliding Mode Observer," *Power Electronics, IEEE Transactions on*, vol. 28, no. 11, pp. 4867-4872, 2013.
- [20] W. Huai, and F. Blaabjerg, "Reliability of Capacitors for DC-Link Applications in Power Electronic Converters: An Overview," *Industry Applications, IEEE Transactions on*, vol. 50, no. 5, pp. 3569-3578, 2014.
- [21] 陈耀红. 高储能密度金属化膜电容器应用性能及其影响因素研究. 博士, 华中科技大学, 2013.
- [22] A. Wechsler, B. C. Mecrow, D. J. Atkinson, J. W. Bennett, and M. Benarous, "Condition Monitoring of DC-Link Capacitors in Aerospace Drives," *Industry Applications, IEEE Transactions on*, vol. 48, no. 6, pp. 1866-1874, 2012.
- [23] J. Yun-Jae, N. Thanh Hai, and L. Dong-Choon, "Condition monitoring of submodule capacitors in modular multilevel converters." pp. 2121-2126.
- [24] L. Kwang-Woon, K. Myungchul, Y. Jangho, L. Kwang-Woon, and Y. Ji-Yoon, "Condition Monitoring of DC-Link Electrolytic Capacitors in Adjustable-Speed Drives," *Industry Applications, IEEE Transactions on*, vol. 44, no. 5, pp. 1606-1613, 2008.

2、主要内容和预期成果（说明研究开发的主要内容，技术关键（难点）以及最终成果形式和对经济社会发展产生的效益）。

## 2.1 主要研究内容

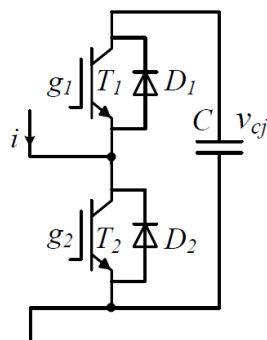


图 2. MMC 子模块拓扑.

本项目中，MMC 的子模块为半桥结构，如图 2 所示，但是提出的方法可用于子模块为其他拓扑的 MMC（若拓扑为其他结构，只需要将方法中的电路模型进行修改即可）。

### 开路故障

当 IGBT 出现开路故障时，对应子模块的电容电压会不断上升。图 3 是一个 24MW 的 MMC 仿真结果，发生开路故障（0.1s）后，故障子模块电容电压不断上升，最终将损坏该模块其他的 IGBT 和电容。为防止二次故障，IGBT 的开路故障须在 40ms 内诊断出来。

本项目拟采用滑模观测器诊断 IGBT 的开路故障。观测器框图如图 4 所示，图中 MMC Submodule 虚线框部分是 MMC 子模块（见图 2）的电路模型， $S$  表示子模块的开关状态，取值见表 I； $i$ 、 $v_c$ 、 $C$  分别为子模块的电流、电容电压和电容值。图 4 中 SMO 虚线框部分是滑模观测器框图，其中  $L_l$  为观测器增益， $sat(x)$  为饱和函数， $\hat{v}_c$  是  $v_c$  的估计值（也称作观测值）。可以证明，当  $L_l$  取值合适且电路工作正常时  $\hat{v}_c$  与  $v_c$  收敛；而当 IGBT 发生开路故障时， $\hat{v}_c$  与  $v_c$  发散。通过这个差异可判断该子模块是否有开路故障。

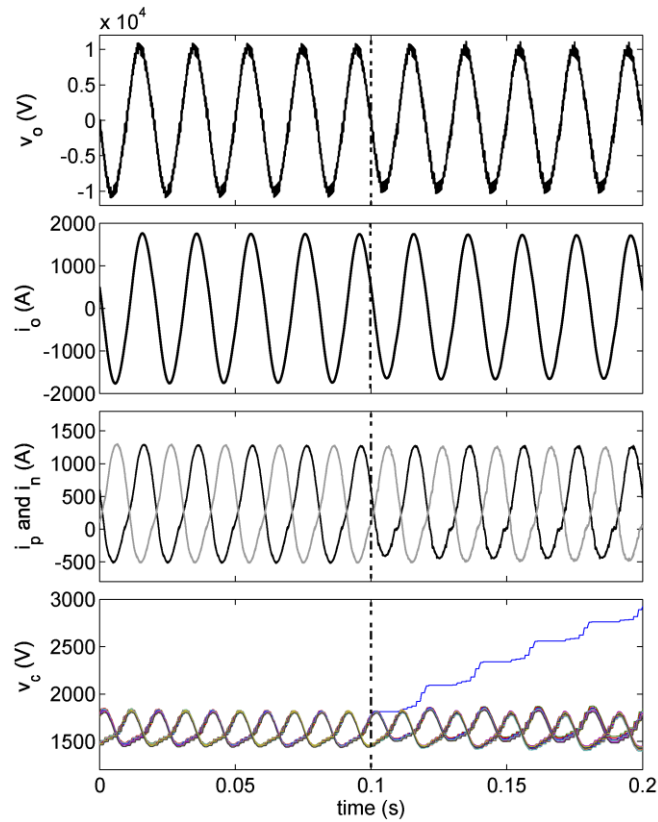


图 3. 24MW MMC 仿真结果, 0.1s 时发生 IGBT 开路故障, 从上至下: 输出电压 ( $v_o$ )、输出电流 ( $i_o$ )、桥臂电流 ( $i_p, i_n$ ) 和子模块电容电压 ( $v_c$ ).

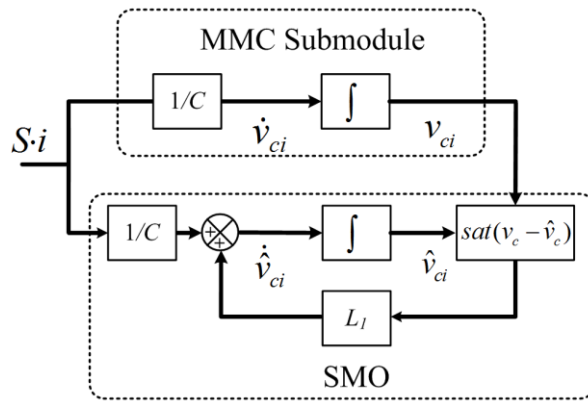


图 4. 估计电容电压的滑模观测器框图.

表 I 子模块开关状态 S 取值表

S	驱动信号
1	$g_1=1, g_2=0$
0	$g_1=0, g_2=1$

## 电容健康状况监测

金属薄膜电容的电容容量会随着其老化而逐渐减小，本项目采用滑模观测器估计电容容量，根据电容容量历史记录来判断其老化程度。

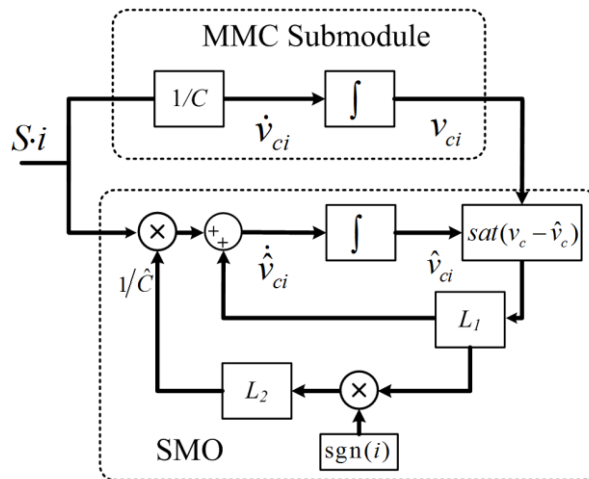


图 5. 估计电容量的滑模观测器框图。

在图 4 的基础上，添加一条估计电容  $C$  的支路，得到滑模观测器图 5，其中  $\hat{C}$  表示电容量的估计值， $\text{sgn}(i)$  表示符号函数，当  $i > 0$ ， $\text{sgn}(i) = 1$ ；当  $i < 0$ ， $\text{sgn}(i) = -1$ 。滑模观测器估计电容值的工作原理如下：若  $\hat{C}$  与  $C$  不一致时， $\hat{v}_c$  与  $v_c$  会有微小的差异，此差异将以反馈的形式修正  $\hat{C}$ ，使  $\hat{C}$  逼近于  $C$ 。 $\hat{C}$  与  $C$  的收敛性亦可以在数学上证明。滑模观测器对外部干扰、建模误差具有较高的免疫性强，确保了  $\hat{C}$  的估计精度。

根据不同子模块电容的老化情况，可以微调各个子模块的使用率：电容老化严重的模块少使用一点，电容较健康的模块多使用一点，最终提高 MMC 系统的电容的整体寿命。

## IGBT 短路故障

IGBT 发生短路故障后，对应 MMC 子模块内半桥直通，电容迅速放电，电容电压急剧下降。图 6 为 MMC 一个子模块 IGBT 短路故障的示意图和仿真波形，子模块上管  $T_1$  在 0.5s 时发生故障，电容电压在短路故障之后迅速降低，仿真结果如图 6 (b) 所示。

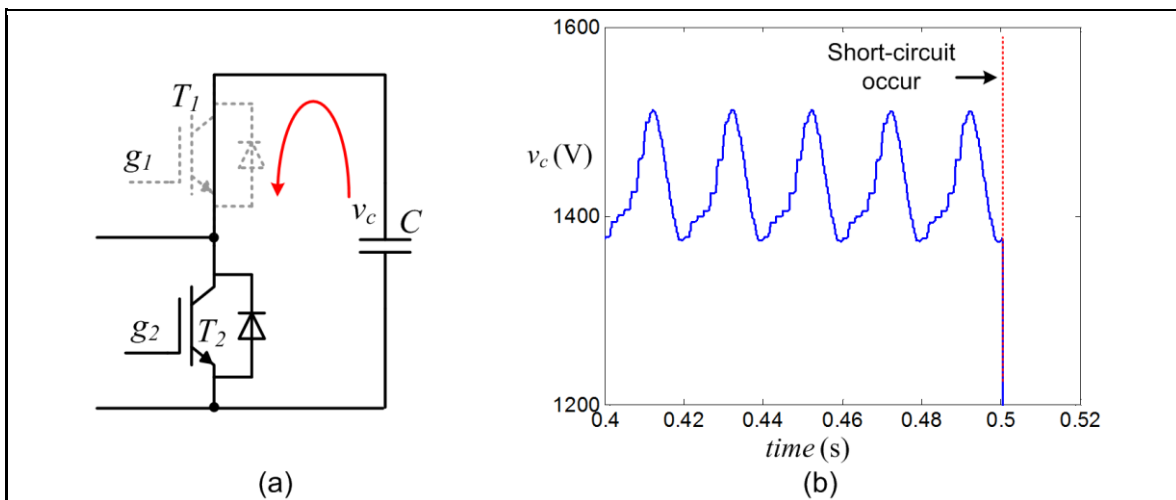


图 6. MMC 子模块 IGBT 短路故障: (a) $T_1$  发生短路故障 (b)电容电压的仿真结果.

利用 MMC 这一特性, 本项目提出一个简单电路诊断 IGBT 的短路故障。所提电路的示意图如图 7 所示, 该电路先采用微分电路分离  $v_c$  的变化率, 当变化率大于一个阈值时, 结合门极信号  $g_1$  即可得知短路故障的具体位置。该电路简单易行, 只需要无源元件、比较器和逻辑门三种元件。该电路可检测出由各种原因造成的 IGBT 短路故障。

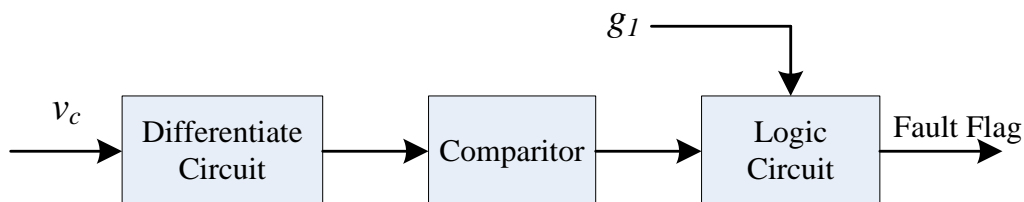


图 7. IGBT 短路故障诊断示意图.

## 2.2 技术关键

1) 在存在测量噪声和建模误差的情况下, 准确地估计 MMC 子模块电容电压和电容值。

状态观测器根据已有的电压、电流和门极信号, 在数字处理器内部对 MMC 子模块进行重构, 估计出电容电压和电容量。然而, 采用的电压、电流信号必然存在测量噪声, 重构时所有的解析模型必然与实际电路存在差异, 这些测量噪声和建模误差将有可能导致估计的电容电压和电容值与其实际值存在差异。如何调整滑模观

测器的参数，最大化减小测量噪声和建模误差对估计值的影响；如何选择合适的阈值，准确快速地诊断开路故障是本项目要解决的关键问题之一。所幸的是，滑模观测器具有部分卡尔曼滤波器特性，对外部干扰的免疫性强，是理想的电容电压和电容值估计算法。

### **2) 准确快速地诊断短路故障并进行电路保护。**

IGBT 短路故障将造成子模块半桥直通，形成大电流，为了防止损坏其他 IGBT，在  $10\mu\text{s}$  之内要将故障 IGBT 定位、关断该子模块内其他 IGBT，并将该子模块从 MMC 主电路中切除，并插入冗余子模块，保证 MMC 的不间断运行。要达到这个目标，一方面需要 IGBT 短路故障诊断电路检测速度快，另一方面需要子模块能根据短路故障信号及时关断其他 IGBT。诊断电路的参数也需要认真设计，消除测量噪声、电路瞬态响应的影响。

### **3) 总结一套有实际工程价值的 MMC 关键元件故障诊断设计方法。**

本项目的最终目标是为 MMC 柔性直流输电系统的关键元件设计一套简单可靠、具有实际工程价值的故障诊断方法。在实验过程中需要测试各方法中重要参数对诊断的准确性和快速性的影响，并分析各参数影响诊断方案的内部机理，修正方案，得到最佳的参数，并以此总结设计方法。

## **2.3 预期成果**

1) 针对 MMC 中故障率最高的元件 IGBT 和电容，提出一整套简单有效的诊断方案。对于子模块中 IGBT 开路故障和电容老化，提出基于滑模观测器的诊断方案。实验验证这些方案的有效性，并总结出行之有效的设计方法。

2) 在 IEEE、IET 国际著名期刊、国际重要会议及国内一级刊物上发表 SCI/EI 论文 2~3 篇，参加国内外学术会议。

3) 申请具有完全自主知识产权的国家发明专利 1~2 个，为今后产业化开发做好技术储备。

### 3、项目实施方案和计划进度安排。

本项目计划2年内完成，研究计划如下：

**2017.1-2017.4** 完善三种故障诊断方案的设计，并通过仿真验证。

**2017.5-2017.8** 设计单个子模块样机主功率电路，控制板等硬件，并开始搭建样机。

**2017.9-2017.12** 完成单个子模块样机调试。在 FPGA 内构建滑模观测器，估计子模块电容电压和电容值。

**2018.1-2018.4** 模拟开路故障，测试开路诊断方法的有效性。整定重要参数对诊断方案鲁棒性和快速性的影响，总结设计方法

**2018.5-2018.8** 制作短路故障诊断电路，并进行实验调试，整定重要参数对诊断方案准确性和快速性的影响。

**2018.9-2018.12** 撰写验收报告，准备验收。

### 4、现有工作基础和条件（包括配套经费、人员配备等情况）。

申请人在诺丁汉大学攻读博士期间（2011.11-2015.07），从事 MMC 功率器件故障诊断的研究工作，对 IGBT 开路和短路故障的原因、已有的诊断方法，以及 MMC 的工作原理有深入的研究，并取得了良好的研究成果。申请人提出了基于滑模观测器和猜想-验证思想的功率器件开路故障诊断方法，该原创性方法的初步结果在 *IEEE Trans. Power Electron.* 发表，并在电力电子国际会议上进行了宣读。为了验证该故障诊断方案，申请人搭建了一台单相 MMC 样机，其图片见图 8。

本项目是对申请人博士课题的深入。原方案只在单个功率器件开路故障时有效，本项目克服上述难点，对多个并发的 IGBT 开路和短路故障能有效诊断出来，且能监测电容的健康状况。本项目已进行了部分的前期预研工作，如各个方案的仿真、参数设计等。

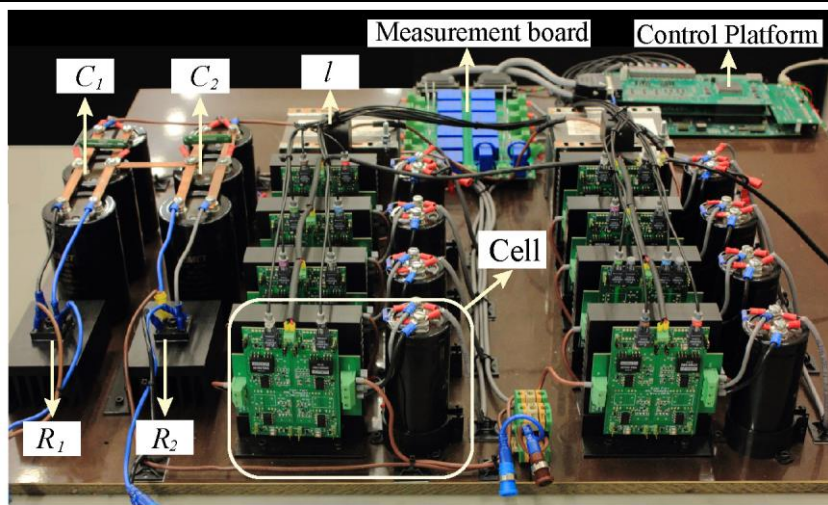


图 8. 申请人在诺丁汉大学搭建的单相 MMC 样机。

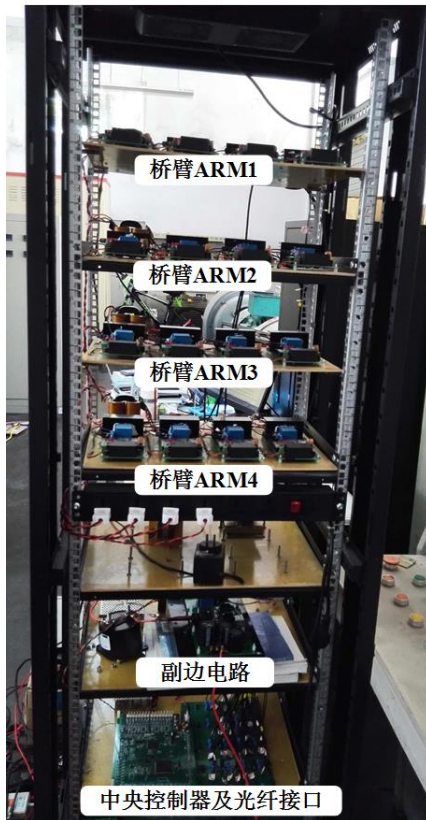


图 9. 申请人所在实验室研制的基于 MMC 的固态变压器样机。

申请人所在的浙江大学电力电子高压高功率实验室，负责人为张军明教授，拥有充分的软件资源，如电路仿真软件 Saber、PLECS，3D 设计软件 Solidworks，热仿真软件 Ansys，电路板绘制软件 Altium Designer 等。课题组具有多年的硬件研发经验，曾与多家公司合作开发产品，从主电路设计、控制到硬件调试、效率优化，



具备一套完整的经验。课题组所依托学科建有先进的电力电子技术国家专业实验室和电力电子技术应用国家工程研究中心，1988 年成为国内首批重点学科。近年来，荣获国家科技进步二等奖等众多奖项。本学科在国际同行中有着较好的学术声誉，与许多国际知名大学、研究机构建立良好的合作关系。实验室具有多年研制大功率电力电子样机能力，曾与多家公司开展项目合作开发产品，具有丰富的工程经验。图 9 是实验室研发的基于 MMC 的固态变压器样机图片。本项目实验所需的三相 MMC 样机可在此样机基础上改装获得，这为项目的实验打下了良好的基础。

申请人所在实验室现有 3 名博士研究生、9 名硕士研究生，这些研究生具备扎实的基础知识和一定的工程能力，可以参与方案仿真、电路设计与调试、数据采集与分析等工作。浙江大学为本项目配套了 20 万的研究经费，分两年发放。这些配套的人员和经费有助于本项目的顺利开展。

<p>本人 声明</p>	<p>我保证以上材料属实，如有不实之处，愿承担一切责任。</p> <p style="text-align: right;">申请人（签名）： 年 月 日</p>
<p>所在单 位审核</p>	<p>申请人以上材料经与原件核对，情况属实。表格所填报内容均已在单位内部进行全信息公示，没有异议。</p> <p style="text-align: right;">申请人单位（盖章） 年 月 日</p>
<p>所在平 台意见</p>	<p>（不在省级留学人员创业园、省重点企业研究院、省级产业集聚区的，无需填写此栏；若是，请注明平台名称：_____）</p> <p style="text-align: right;">（盖章） 年 月 日</p>
<p>市人力 社保局 或归口 管理部门 审查 意见</p>	<p style="text-align: right;">负责人签字： 年 月 日 单位（盖章）</p>
<p>“钱江人 才计划” 管理办 公室审 查意见</p>	<p style="text-align: right;">负责人签字： 年 月 日 单位（盖章）</p>

## 附件 3

### **C、D 类项目申报附件材料清单**

一、各类论文、著作、专利、奖项等复印件各 1 份，与申请表一同简装成册（注：著作类只需复印封面、目录、前三页及封底）；

二、申请者有效护照（验护照出入境记录）复印件 1 份；

三、浙江省户籍证明（身份证或户口簿）、浙江省留学人员工作证、居住证复印件各 1 份（应邀来本省讲学或进行咨询服务的留学人员除外）；

四、与现工作单位签订的工作合同或自主创业公司营业执照、学位证、职称证复印件各 1 份；

五、留学人员资格认定材料复印件 1 份，可以是下列材料之一：

1. 人力社保部门出具的《留学人员工作证》；
2. 国家教育部出具的《国外学历学位认证书》；
3. 我国驻外使（领）馆出具的《留学回国人员证明》。

# IEEE TRANSACTIONS ON POWER ELECTRONICS

A PUBLICATION OF THE IEEE POWER ELECTRONICS SOCIETY



NOVEMBER 2013

VOLUME 28

NUMBER 11

ITPEE8

(ISSN 0885-8993)

---

## LETTERS

Fault Detection for Modular Multilevel Converters Based on Sliding Mode Observer .....	4867
.....S. Shao, P. W. Wheeler, J. C. Clare, and A. J. Watson	
An Inner Current Suppressing Method for Modular Multilevel Converters .....	4873
.....Z. Li, P. Wang, Z. Chu, H. Zhu, Y. Luo, and Y. Li	
$\Gamma$ -Z-Source Inverters .....	4880
.....P. C. Loh, D. Li, and F. Blaabjerg	
An Improved Soft-Switching Buck Converter With Coupled Inductor .....	4885
.....L. Jiang, C. C. Mi, S. Li, C. Yin, and J. Li	
Quasi-Resonant Boost-Half-Bridge Converter With Reduced Turn-Off Switching Losses for 16 V Fuel Cell Application .....	4892
.....C. Park and S. Choi	
Soft-Switched Dual-Input DC-DC Converter Combining a Boost-Half-Bridge Cell and a Voltage-Fed Full-Bridge Cell .....	4897
.....Z. Zhang, O. C. Thomsen, and M. A. E. Andersen	
Accelerated Simulation of High-Fidelity Models of Supercapacitors Using Waveform Relaxation Techniques .....	4903
.....S. Moayedi, F. Cingöz, and A. Davoudi	
Nonlinear Current Control for Power Electronic Converters: IC Design Aspects and Implementation .....	4910
.....M. Nikolić, R. Enne, B. Goll, and H. Zimmermann	

---

## REGULAR PAPERS

### *High Power Converters*

Enhancement of Commutation Reliability of an HVDC Inverter by Means of an Inductive Filtering Method .....	4917
.....Y. Li, F. Liu, L. Luo, C. Rehtanz, and Y. Cao	
Cascaded Multilevel Converter-Based Transmission STATCOM: System Design Methodology and Development of a 12 kV $\pm$ 12 MVar Power Stage .....	4930
.....B. Gultekin and M. Ermis	
Variable Switching Frequency PWM for Three-Phase Converters Based on Current Ripple Prediction .....	4951
.....D. Jiang and F. (Fred) Wang	
Isolated Three-Phase High Power Factor Rectifier Based on the SEPIC Converter Operating in Discontinuous Conduction Mode .....	4962
.....G. Tibola and I. Barbi	
CCTT-Core Split-Winding Integrated Magnetic for High-Power DC-DC Converters .....	4970
.....K. J. Hartnett, J. G. Hayes, M. G. Egan, and M. S. Rylko	

(Contents Continued on Page 4865)



---

*Power Quality & Utilities*

Advantages and Challenges of a Type-3 PLL . . . . . *S. Golestan, M. Monfared, F. D. Freijedo, and J. M. Guerrero* 4985

A Novel RPV (Reactive-Power-Variation) Antiislanding Method Based on Adapted Reactive Power Perturbation . . . . .  
. . . . . *Y. Zhu, D. Xu, N. He, J. Ma, J. Zhang, Y. Zhang, G. Shen, and C. Hu* 4998

*EMI/EMC*

New Random PWM Technique for a Full-Bridge DC/DC Converter With Harmonics Intensity Reduction and Considering Efficiency . . . . . *Y.-S. Lai and B.-Y. Chen* 5013

*Renewable Energy*

Mitigation of Lower Order Harmonics in a Grid-Connected Single-Phase PV Inverter . . . . . *A. Kulkarni and V. John* 5024

Adaptive Voltage Control of the DC/DC Boost Stage in PV Converters With Small Input Capacitor . . . . .  
. . . . . *A. Urtasun, P. Sanchis, and L. Marroyo* 5038

A High Step-Up Three-Port DC–DC Converter for Stand-Alone PV/Battery Power Systems . . . . .  
. . . . . *Y.-M. Chen, A. Q. Huang, and X. Yu* 5049

Modular Multilevel Inverter with New Modulation Method and Its Application to Photovoltaic Grid-Connected Generator . . . . .  
. . . . . *J. Mei, B. Xiao, K. Shen, L. M. Tolbert, and J. Y. Zheng* 5063

An Optimal Control Method for Photovoltaic Grid-Tied-Interleaved Flyback Microinverters to Achieve High Efficiency in Wide Load Range . . . . .  
. . . . . *Z. Zhang, X.-F. He, and Y.-F. Liu* 5074

Theoretical and Experimental Analysis of an MPP Detection Algorithm Employing a Single-Voltage Sensor Only and a Noisy Signal . . . . .  
. . . . . *E. Dallago, D. G. Finarelli, U. P. Gianazza, A. L. Barnabei, and A. Liberale* 5088

Integration and Operation of a Single-Phase Bidirectional Inverter With Two Buck/Boost MPPTs for DC-Distribution Applications . . . . .  
. . . . . *T.-F. Wu, C.-L. Kuo, K.-H. Sun, Y.-K. Chen, Y.-R. Chang, and Y.-D. Lee* 5098

Dynamic Stability of a Microgrid With an Active Load . . . . . *N. Bottrell, M. Prodanovic, and T. C. Green* 5107

*Low Power Converters*

Variable Delay Time Method in the Phase-Shifted Full-Bridge Converter for Reduced Power Consumption Under Light Load Conditions . . . . .  
. . . . . *D.-Y. Kim, C.-E. Kim, and G.-W. Moon* 5120

Secondary-Side Phase-Shift-Controlled ZVS DC/DC Converter With Wide Voltage Gain for High Input Voltage Applications . . . . .  
. . . . . *W. Li, S. Zong, F. Liu, H. Yang, X. He, and B. Wu* 5128

An Isolated Output-Feedback Scheme With Minimized Standby Power for SMPS . . . . . *C.-J. Chang and C.-L. Chen* 5140

A Unified Analytical Modeling of the Interleaved Pulse Width Modulation (PWM) DC–DC Converter and Its Applications . . . . .  
. . . . . *S. Zhang and X. Yu* 5147

92% High Efficiency and Low Current Mismatch Interleaving Power Factor Correction Controller With Variable Sampling Slope and Automatic Loading Detection Techniques . . . . .  
. . . . . *Y.-P. Su, C.-Y. Chen, C.-L. Ni, Y.-C. Kang, Y.-T. Chen, J.-C. Tsai, K.-H. Chen, S.-M. Wang, C.-C. Liang, C.-A. Ho, and T.-H. Yu* 5159

Low-Noise Switched-Capacitor Power Converter With Adaptive On-Chip Surge Suppression and Preemptive Timing Control . . . . .  
. . . . . *C. Zheng, I. Chowdhury, and D. Ma* 5174

Stacked Switched Capacitor Energy Buffer Architecture . . . . . *M. Chen, K. K. Afridi, and D. J. Perreault* 5183

A Family of Single-Stage Switched-Capacitor–Inductor PWM Converters . . . . . *Y. Ye and K. W. E. Cheng* 5196

A Bridgeless Boost Rectifier for Low-Voltage Energy Harvesting Applications . . . . . *H. Wang, Y. Tang, and A. Khaligh* 5206

A Class-*E* RF Power Amplifier With a Flat-Top Transistor-Voltage Waveform . . . . . *A. Mediano and N. O. Sokal* 5215

Analysis and Design of Class-*E* Power Amplifier With MOSFET Parasitic Linear and Nonlinear Capacitances at Any Duty Ratio . . . . .  
. . . . . *M. Hayati, A. Lotfi, M. K. Kazimierczuk, and H. Sekiya* 5222

Load Detection Model of Voltage-Fed Inductive Power Transfer System . . . . .  
. . . . . *Z.-H. Wang, Y.-P. Li, Y. Sun, C.-S. Tang, and X. Lv* 5233

*Control in Power Electronics*

Avoiding a Voltage Sag Detection Stage for a Single-Phase Multilevel Rectifier by Using Control Theory Considering Physical Limitations of the System . . . . .  
. . . . . *N. Visairo, C. Nunez, J. Lira, and I. Lazaro* 5244

Control Scheme With Voltage Support Capability for Distributed Generation Inverters Under Voltage Sags . . . . .  
. . . . . *J. Miret, A. Camacho, M. Castilla, L. García de Vicuña, and J. Matas* 5252

Predictive Fast DSP-Based Current Controller for a 12-Pulse Hybrid-Mode Thyristor Rectifier . . . . .  
. . . . . *Z. Damin, W. Shitao, Z. Fengwu, W. Lujun, and L. Zhengyu* 5263

---

# Letters

## Fault Detection for Modular Multilevel Converters Based on Sliding Mode Observer

Shuai Shao, Patrick W. Wheeler, Jon C. Clare, and Alan J. Watson

**Abstract**—This letter presents a fault detection method for modular multilevel converters which is capable of locating a faulty semiconductor switching device in the circuit. The proposed fault detection method is based on a sliding mode observer (SMO) and a switching model of a half-bridge, the approach taken is to conjecture the location of fault, modify the SMO accordingly and then compare the observed and measured states to verify, or otherwise, the assumption. This technique requires no additional measurement elements and can easily be implemented in a DSP or microcontroller. The operation and robustness of the fault detection technique are confirmed by simulation results for the fault condition of a semiconductor switching device appearing as an open circuit.

**Index Terms**—Fault detection, modular multilevel converter (MMC), sliding mode observer (SMO), switching model.

### I. INTRODUCTION

THE modular multilevel converter (MMC) has drawn considerable interest, as it offers very attractive features [1]–[4]:

- 1) modular construction with scalable, manufacturable, standardised cells (half-bridge);
- 2) submodules are fed by floating dc capacitors, no multi-pulse transformer is required;
- 3) high power and high voltage capability, extendable by adding additional cells;
- 4) flexible control of the voltage level and simple realization of redundancy if required.

Fault detection is an important issue for an MMC. When an open-circuit fault occurs, the output voltage and current are distorted, moreover, the voltages of the dc floating capacitors will keep increasing, leading to further, vast destruction. Therefore, it is vital to locate the fault after its occurrence and take measures such as bypassing the faulty cell to reconfigure the MMC.

Manuscript received June 27, 2012; revised November 6, 2012 and December 24, 2012; accepted January 15, 2013. Date of current version May 3, 2013. Recommended for publication by Associate Editor J. Jatskevich.

The authors are with the Power Electronics, Machines and Control Group, School of Electrical and Electronic Engineering, University of Nottingham, Nottingham NG7 2RD, U.K. (e-mail: eexss21@nottingham.ac.uk; Pat.Wheeler@nottingham.ac.uk; Jon.Clare@nottingham.ac.uk; Alan.watson@nottingham.ac.uk).

Color versions of one or more of the figures in this paper are available online at <http://ieeexplore.ieee.org>.

Digital Object Identifier 10.1109/TPEL.2013.2242093

Given the large numbers of identical cells (half-bridge) and the symmetrical structure of the converter, the process of fault location in an MMC is challenging if significant extra cost is to be avoided. An effective but inefficient way to detect faults is to add additional sensors to each semiconductor switching device [5], to each cell [6], or to use a gate drive module capable of detecting faults and providing feedback [7]. These additional sensors and signals increase not only the cost but also the implementation complexity. Some conventional fault detection methods for voltage source converters (VSCs), such as the calculation of the output current trajectory using Park's Vector [8], [9], or comparison of the actual ac voltage and the reference quantity [10] are, however, not suitable for an MMC, as there is not enough information present to locate the fault.

Fault diagnosis methods for a cascaded H-bridge (CHB) are applicable to an MMC because of the similar structure. The authors in [11] presented a detection approach for a CHB multilevel converter, which analyzes magnitude of the switching frequency component ( $v_s$ ) of the output phase voltage:  $v_s$  becomes significantly larger after the occurrence of a fault due to the imbalanced cancellation of the switching frequency harmonics. The faulty cell can be located according to the angle of  $v_s$  [11]. However, the faulty switching device cannot be located, and it is complex to implement and easy to get the wrong diagnosis in transient operation. In [12], the authors proposed an artificial intelligence (AI)-based algorithm to detect the fault of a CHB, the major drawbacks are the accuracy (only 76% in some cases) and the long training time required for the circuit and all the fault scenarios.

This letter proposes a sliding mode observer (SMO)-based fault detection method for an MMC. The method uses the converter arm currents and the cell capacitor voltages as the inputs, which are already available as measurement inputs to the control system, no additional sensors are required. Using this method not only the faulty cell, but also the faulty switching device can be located. Moreover, inherited from the easy implementation and robustness of the SMO [13]–[15], this method has good immunity to conditions such as transient operation, degradation of capacitance over time, and measurement inaccuracies.

### II. SWITCHING MODEL OF A HALF-BRIDGE

A half-bridge (see Fig. 1) is the basic cell of an MMC. In order to diagnose an open-circuit fault, it is essential to identify the characteristics of a half-bridge as observed from its dc-side and ac-side both in normal and fault conditions.

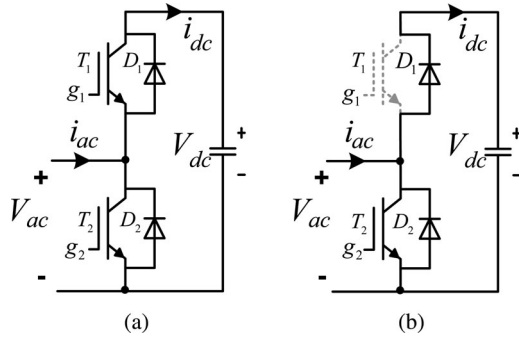


Fig. 1. Switching model of half-bridge. (a) Normal condition. (b) Fault condition (an open-circuit fault at  $T_1$ ).

TABLE I  
SWITCHING STATE  $S$  IN NORMAL CONDITION

$S$	Driving signals
1	$g_1 = 1, g_2 = 0$
0	$g_1 = 0, g_2 = 1$

$g_1$  and  $g_2$  in Fig. 1 are the gate signals for the switches, and are complementary. When the gate signal is 1, the corresponding switch turns ON; when it is 0, the corresponding switch turns OFF.

The analysis assumes ideal devices and instantaneous commutation. The fault detection method is, however, robust against nonideal device characteristics. This is verified in the all of the simulation results where generous values of 5 V and  $1 \mu\text{s}$  are included for the device voltage drop and dead-time delay respectively.

1) *Normal (Fault-Free) Condition:* As shown in Fig. 1(a), when  $g_1 = 1, g_2 = 0$ ,  $T_1$  is ON and  $T_2$  is OFF, thus  $V_{ac} = V_{dc}$ ,  $i_{dc} = i_{ac}$ ; alternatively, when  $g_1 = 0, g_2 = 1$ ,  $V_{ac} = 0$ ,  $i_{dc} = 0$ . Therefore, the relationship between the ac-side and dc-side voltages and currents can be calculated as

$$\begin{cases} V_{ac} = S \cdot V_{dc} \\ i_{dc} = S \cdot i_{ac} \end{cases} \quad (1)$$

where  $S$  is the switching state given by Table I.

2) *Fault Condition:* In the fault condition (one open-circuit fault of the switch), the switching models can still be described as (1), but the switching states  $S$  have to be modified.

Consider the half-bridge with an open circuit fault at  $T_1$ , as shown in Fig. 1(b). When  $g_1 = 1$ ,  $i_{ac} < 0$ ,  $i_{ac}$  is forced to go through  $D_2$  instead of  $T_1$  as the result of the open-circuit fault. Thus, the switching state  $S$  should be changed from 1 to 0. For all other conditions, the half-bridge operates just as normal.

When the open-circuit fault occurs on  $T_2$ , the switching state can be modified in a similar way. Table II demonstrates the modifications of switching states of a faulty half-bridge.

### III. SLIDING MODE OBSERVER

An observer is a contrivance designed from a real system, generally in the same mathematical form as the original system, so as to estimate its internal state [13], [16]. The SMO

TABLE II  
SWITCHING STATE  $S$  IN FAULT CONDITION

Location of the fault	Condition	Switching State	
		Normal	Fault
$T_1$	$g_1 = 1, i_{ac} < 0$	1	$S_F = 0$
	Other conditions	S	$S_F = S$
$T_2$	$g_2 = 1, i_{ac} > 0$	0	$S_F = 1$
	Other conditions	S	$S_F = S$

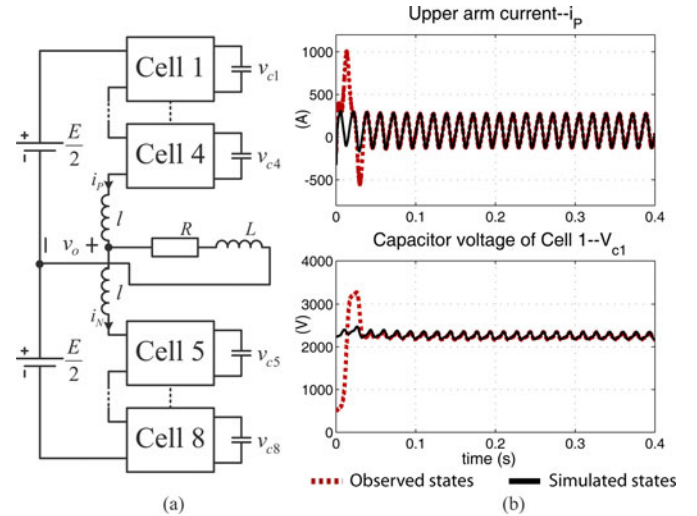


Fig. 2. (a) Eight cell MMC circuit (each cell represents a half-bridge). (b) SMO simulated results in normal conditions.

uses high-gain feedback in the observer vector (normally in the form of a high-frequency switching function, for example the saturation function of an observed-measured error, as (3) and (4) present) to force the observed output to converge to the actual output [13], [15]. The SMO offers desirable features such as robustness to parameter uncertainty and insensitivity to measurement noise [13]–[15], [17]. With simple realization, the SMO can be implemented in the field-programmable gate array (FPGA) [16], [17].

Based on [16] and [18], the SMO can be developed for a single-phase eight cell MMC as shown in Fig. 2(a). The equations which characterize the upper arm can be expressed as

$$\begin{aligned} \frac{di_P}{dt} &= -\frac{1}{l} \left( S_1 v_{c1} + S_2 v_{c2} + S_3 v_{c3} + S_4 v_{c4} + v_o - \frac{E}{2} \right) \\ \frac{dv_{ci}}{dt} &= \frac{1}{C} S_i i_P \quad (i = 1, 2, 3, 4) \end{aligned} \quad (2)$$

where  $l$  is the arm inductance, as shown in Fig. 2(a),  $C$  is the dc-capacitance,  $v_{c1}, \dots, v_{c4}$  are the capacitor voltages of cell 1 to cell 4, respectively,  $S_1, \dots, S_4$  are the corresponding switching states of the half-bridges given by Table I.

If  $i_P$  and one of the capacitor voltages ( $v_{c1}, \dots, v_{c4}$ , we consider  $v_{c1}$  in this case) are selected to be observed, then the



SMO equations are

$$\begin{aligned} \frac{d\hat{i}_P}{dt} &= -\frac{1}{l} \left( S_1 \hat{v}_{c1} + S_2 v_{c2} + S_3 v_{c3} + S_4 v_{c4} \right. \\ &\quad \left. + v_o - \frac{E}{2} \right) - L_1 \text{sat}(\hat{i}_P - i_P) \\ \frac{d\hat{v}_{c1}}{dt} &= \frac{1}{C} S_1 \hat{i}_P - L_2 \text{sat}(-l S_1 L_1 \text{sat}(\hat{i}_P - i_P)) \end{aligned} \quad (3)$$

where  $\hat{i}_P$  and  $\hat{v}_{c1}$  denote the observed states associated with the actual states  $i_P$  and  $v_{c1}$ ;  $L_1 \text{sat}(\hat{i}_P - i_P)$  and  $L_2 \text{sat}(-l S_1 L_1 \text{sat}(\hat{i}_P - i_P))$  comprise the observer vector, whose derivations are detailed in [16], [18];  $L_1$  and  $L_2$  are the observer gains (large constant, for example 20000) to guarantee the sliding mode;  $\text{sat}(x)$  is the saturation function, which is defined as

$$\text{sat}(x) = \begin{cases} 1 & x \geq 1 \\ x & -1 < x < 1 \\ -1 & x \leq -1 \end{cases} \quad (4)$$

According to the analysis of [16], the system described in (3) is observable when  $S_1 = 1$ .

The MMC circuit is simulated using Simulink/PLECS. The observed and actual simulated states are shown in Fig. 2(b), from which one can see that  $\hat{i}_P$  and  $\hat{v}_{c1}$  accurately match  $i_P$  and  $v_{c1}$ , respectively. The lower arm current and capacitor voltage can be observed in the same way.

#### IV. FAULT DETECTION ON AN MMC USING SLIDING MODE OBSERVER

The basic idea of this detection method is to compare the observed state and the actual simulated state of the MMC, and if they are different for a predefined period of time, then a fault has occurred, and a procedure including assumption, modification, and judgement to locate the open-circuit fault begins.

The fault detection systems consists of two modes, as specified in Fig. 3. The process of each mode is detailed as follows. Consider the upper arm of the MMC circuit in Fig. 2(a), and suppose that it initially operates in normal, steady conditions.

##### A. Monitor Mode

The aim of this mode is to determine whether the MMC is operating normally.  $i_P$  and one of the any capacitor voltages (for example  $v_{c1}$ ) are observed.

If  $|\hat{i}_P - i_P| \geq I_{\text{Threshold}}$ , where  $I_{\text{Threshold}}$  is the threshold value of current error, and it lasts for 700 time steps ( $2 \mu\text{s}$  per step), then an open-circuit fault has occurred. We denote this moment as  $t_0$  and go to the *detection mode*; else, repeat the *monitor mode*. Note that the decision of fault occurrence is made only if the observed-simulated error ( $|\hat{i}_P - i_P|$ ) lasts for a period of time (700 time-steps in this letter, empirical value), this is useful to prevent ‘‘false positives’’, as the measurement noise may also lead to  $|\hat{i}_P - i_P| \geq I_{\text{Threshold}}$ .

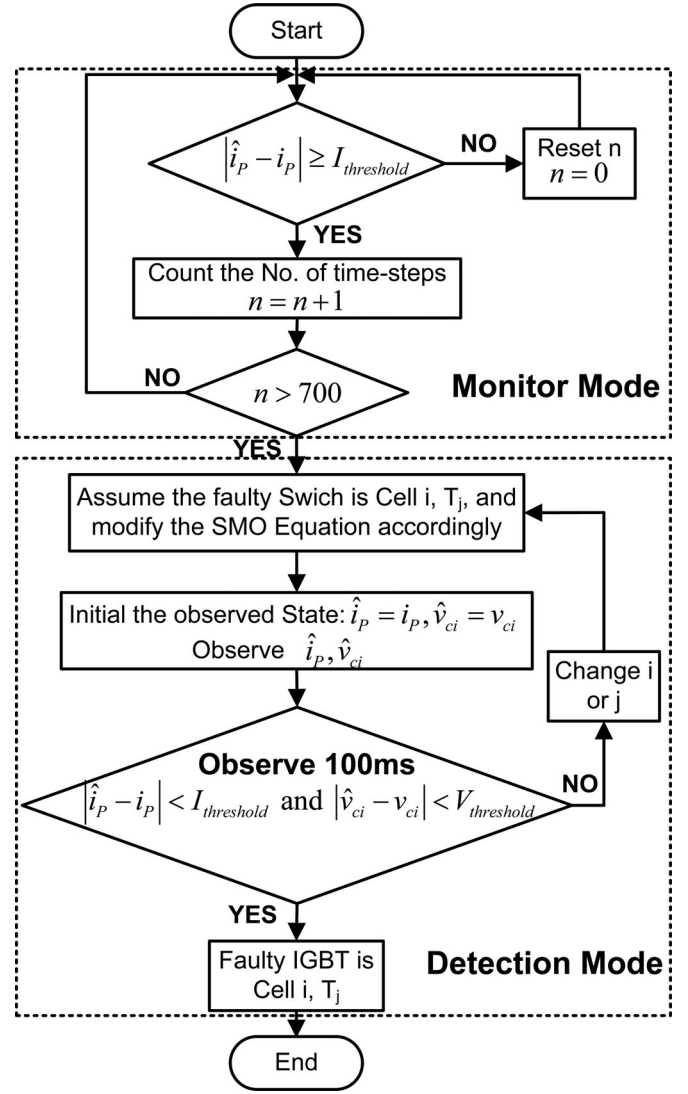


Fig. 3. Flowchart of the fault detection system.

##### B. Detection Mode

The aim of this mode is to locate the open-circuit after its occurrence.

*D1 (Assumption and Modification):* Set the assumed faulty switch as *Cell*  $i$  ( $i = 1, 2, 3, 4$ ),  $T_j$  ( $j = 1, 2$ ), modify  $S_i$  (replace  $S$  with  $S_F$ ) of SMO in (3) based on the Table II, set  $\hat{i}_P(t_0) = i_P(t_0)$ ,  $\hat{v}_{ci}(t_0) = v_{ci}(t_0)$ , and observe  $i_P$  and  $v_{ci}$ . For example, if the assumed faulty switch is *Cell* 4,  $T_1$ , then  $i_P$  and  $v_{c4}$  are observed, and the observer equations are

$$\begin{aligned} \frac{d\hat{i}_P}{dt} &= -\frac{1}{l} \left( S_{4(F)} \hat{v}_{c4} + S_1 v_{c1} + S_2 v_{c2} + S_3 v_{c3} \right. \\ &\quad \left. + v_o - \frac{E}{2} \right) - L_1 \text{sat}(\hat{i}_P - i_P) \\ \frac{d\hat{v}_{c4}}{dt} &= \frac{1}{C} S_{4(F)} \hat{i}_P - L_2 \text{sat}(-l S_{4(F)} L_1 \text{sat}(\hat{i}_P - i_P)). \end{aligned} \quad (5)$$

*D2 (Judgement):* If  $|\hat{i}_P - i_P| < I_{\text{Threshold}}$  and  $|\hat{v}_{ci} - v_{ci}| < V_{\text{Threshold}}$ , where  $V_{\text{Threshold}}$  is the threshold value of voltage



# IEEE TRANSACTIONS ON POWER ELECTRONICS

A PUBLICATION OF THE IEEE POWER ELECTRONICS SOCIETY



MAY 2016

VOLUME 31

NUMBER 5

ITPEE8

(ISSN 0885-8993)

## LETTERS

LLC Resonant Converter With Semiactive Variable-Structure Rectifier (SA-VSR) for Wide Output Voltage Range Application . . . . .	
..... <i>H. Wu, Y. Li, and Y. Xing</i>	3389
An Enhanced Control Algorithm for Improving the Light-Load Efficiency of Noninverting Synchronous Buck–Boost Converters . . . . .	
..... <i>D.-H. Kim and B.-K. Lee</i>	3395

## PAPERS

### *High Power Converters*

An Integrated Inductor for Parallel Interleaved Three-Phase Voltage Source Converters . . . . .	
..... <i>G. Gohil, L. Bede, R. Teodorescu, T. Kerekes, and F. Blaabjerg</i>	3400
Modeling and Analysis of Class EF and Class E/F Inverters With Series-Tuned Resonant Networks . . . . .	
..... <i>S. Aldhafer, D. C. Yates, and P. D. Mitcheson</i>	3415
Wide Load Range ZVS Three-Level DC–DC Converter: Four Primary Switches, Capacitor Clamped, Two Secondary Switches, and Smaller Output Filter Volume . . . . .	
..... <i>Y. Shi and X. Yang</i>	3431
Wideband Mechanism Model and Parameter Extracting for High-Power High-Voltage High-Frequency Transformers . . . . .	
..... <i>C. Liu, L. Qi, X. Cui, Z. Shen, and X. Wei</i>	3444
Theory and Experiment on an Optimal Carrier Frequency of a Modular Multilevel Cascade Converter With Phase-Shifted PWM . . . . .	
..... <i>F. Sasongko, K. Sekiguchi, K. Oguma, M. Hagiwara, and H. Akagi</i>	3456
Closed-Form Oriented Modeling and Analysis of Wireless Power Transfer System With Constant-Voltage Source and Load . . . . .	
..... <i>Y. Zhang, K. Chen, F. He, Z. Zhao, T. Lu, and L. Yuan</i>	3472
Analysis of High-Power Switched-Capacitor Converter Regulation Based on Charge-Balance Transient-Calculation Method . . . . .	
..... <i>B. Wu, S. Li, K. M. Smedley, and S. Singer</i>	3482
A Three-Phase Multilevel Hybrid Switched-Capacitor PWM PFC Rectifier for High-Voltage-Gain Applications . . . . .	
..... <i>D. F. Cortez and I. Barbi</i>	3495

### *Power Quality & Utilities*

Investigation of Transformer-Based Solutions for the Reduction of Inrush and Phase-Hop Currents . . . . .	
..... <i>R. Dogan, S. Jazebi, and F. de León</i>	3506
Small-Signal Modeling, Stability Analysis and Design Optimization of Single-Phase Delay-Based PLLs . . . . .	
..... <i>S. Golestan, J. M. Guerrero, A. Vidal, A. G. Yepes, J. Doval-Gandoy, and F. D. Freijedo</i>	3517
DC Microgrids—Part II: A Review of Power Architectures, Applications, and Standardization Issues . . . . .	
..... <i>T. Dragičević, X. Lu, J. C. Vasquez, and J. M. Guerrero</i>	3528

### *Renewable Energy*

High-Gain Single-Stage Boosting Inverter for Photovoltaic Applications . . . . .	
..... <i>A. Abramovitz, B. Zhao, and K. M. Smedley</i>	3550
An Islanding Detection Method for Inverter-Based Distributed Generators Based on the Reactive Power Disturbance . . . . .	
..... <i>X. Chen and Y. Li</i>	3559

(Contents Continued on Back Cover)



---

Enhancing Microinverter Energy Capture With Submodule Differential Power Processing .....	3575
..... S. Qin, C. B. Barth, and R. C. N. Pilawa-Podgurski	
Adaptive $Q$ - $V$ Scheme for the Voltage Control of a DFIG-Based Wind Power Plant .....	3586
..... J. Kim, J.-K. Seok, E. Muljadi, and Y. C. Kang	
Comparison of Dynamic Characteristics Between Virtual Synchronous Generator and Droop Control in Inverter-Based Distributed Generators .....	3600
..... J. Liu, Y. Miura, and T. Ise	
Highly Accurate Derivatives for $LCL$ -Filtered Grid Converter With Capacitor Voltage Active Damping .....	3612
..... Z. Xin, P. C. Loh, X. Wang, F. Blaabjerg, and Y. Tang	
<i>Low Power Converters</i>	
A ZVS Grid-Connected Full-Bridge Inverter With a Novel ZVS SPWM Scheme .....	3626
..... Y. Chen, D. Xu, J. Xi, G. Hu, C. Du, Y. Li, and M. Chen	
Hybrid PWM-Resonant Converter for Electric Vehicle On-Board Battery Chargers .....	3639
..... I.-O. Lee	
Pseudo-Constant Switching Frequency in On-Time Controlled Buck Converter with Predicting Correction Techniques .....	3650
..... W.-C. Chen, H.-C. Chen, M.-W. Chien, Y.-W. Chou, K.-H. Chen, Y.-H. Lin, T.-Y. Tsai, S.-R. Lin, and C.-C. Lee	
VRSPV Soft-Start Strategy and AICS Technique for Boost Converters to Improve the Start-Up Performance .....	3663
..... S. Fan, Z. Xue, Z. Guo, Y. Wang, and L. Geng	
Linear Regulator Design Considerations of the Serial Linear-Assisted Switching Converter Used as Envelope Amplifier .....	3673
..... M. Liu, D. Zhang, and Z. Zhou	
A Series-Stacked Power Delivery Architecture With Isolated Differential Power Conversion for Data Centers .....	3690
..... E. Candan, P. S. Shenoy, and R. C. N. Pilawa-Podgurski	
<i>Power Electronic Drives</i>	
Single-Phase to Three-Phase Converters With Two Parallel Single-Phase Rectifiers and Reduced Switch Count .....	3704
..... N. Rocha, Í. A. Cavalcanti de Oliveira, E. C. de Menezes, C. B. Jacobina, and J. Artur Alves Dias	
Synchronous Switching of Non-Line-Start Permanent Magnet Synchronous Machines From Inverter to Grid Drives .....	3717
..... R. Ni, D. Xu, G. Wang, G. Zhang, and C. Li	
Feedback Linearization Direct Torque Control With Reduced Torque and Flux Ripples for IPMSM Drives .....	3728
..... Y.-S. Choi, H. H. Choi, and J.-W. Jung	
A New Predictive Direct Torque Control Method for Improving Both Steady-State and Transient-State Operations of the PMSM .....	3738
..... M. H. Vafaie, B. M. Dehkordi, P. Moallem, and A. Kiyounarsi	
<i>Passive Components &amp; Materials</i>	
Loss Modeling of Coupled Stripline Microinductors in Power Supply on Chip Applications .....	3754
..... C. Feeney, N. Wang, S. Kulkarni, Z. Pavlović, C. Ó Mathúna, and M. Duffy	
High-Frequency Behavioral Ring Core Inductor Model .....	3763
..... C. Cuellar, N. Idir, and A. Benabou	
<i>Lighting Applications</i>	
A Scalable $N$ -Color LED Driver Using Single Inductor Multiple Current Output Topology .....	3773
..... K. Modepalli and L. Parsa	
<i>Discrete &amp; Integrated Semiconductors</i>	
IGBT Junction Temperature Measurement via Peak Gate Current .....	3784
..... N. Baker, S. Munk-Nielsen, F. Iannuzzo, and M. Liserre	
<i>Diagnostics in Power Electronics</i>	
Robustness Analysis and Experimental Validation of a Fault Detection and Isolation Method for the Modular Multilevel Converter .....	3794
..... S. Shao, A. J. Watson, J. C. Clare, and P. W. Wheeler	
Open-Circuit Fault-Tolerant Control for Outer Switches of Three-Level Rectifiers in Wind Turbine Systems .....	3806
..... J.-S. Lee and K.-B. Lee	
An Open-Switch Fault Diagnosis Method for Single-Phase PWM Rectifier Using a Model-Based Approach in High-Speed Railway Electrical Traction Drive System .....	3816
..... B. Gou, X. Ge, S. Wang, X. Feng, J. B. Kuo, and T. G. Habetler	
<i>Control in Power Electronics</i>	
Minimizing Effect of Input Filter Capacitor in a Digital Boundary Conduction Mode Power Factor Corrector Based on Time-Domain Analysis .....	3827
..... J.-W. Kim and G.-W. Moon	
Continuous Space Vector Modulation for Symmetrical Six-Phase Drives .....	3837
..... D. Glose and R. Kennel	
Small-Signal Modeling of $I_2$ Average Current Mode Control .....	3849
..... S. He, J. Y. Hung, and R. M. Nelms	
A Novel SVPWM Algorithm for Five-Level Active Neutral-Point-Clamped Converter .....	3859
..... Z. Liu, Y. Wang, G. Tan, H. Li, and Y. Zhang	
Estimation of Single-Phase Grid Voltage Parameters With Zero Steady-State Error .....	3867
..... Z. Dai, W. Lin, and H. Lin	
An Improved Grid-Voltage Feedforward Strategy for High-Power Three-Phase Grid-Connected Inverters Based on the Simplified Repetitive Predictor .....	3880
..... Q. Yan, X. Wu, X. Yuan, and Y. Geng	
Pseudo-Derivative-Feedback Current Control for Three-Phase Grid-Connected Inverters With $LCL$ Filters .....	3898
..... J. Wang, J. D. Yan, and L. Jiang	
A Sensorless Implementation of the Parabolic Current Control for Single-Phase Stand-Alone Inverters .....	3913
..... L. Zhang, R. Born, B. Gu, B. Chen, C. Zheng, X. Zhao, and J.-S. Lai	
A Simplified Equivalent Circuit Model of Series Resonant Converter .....	3922
..... S. Tian, F. C. Lee, and Q. Li	
Comparative Performance Evaluation of Orthogonal-Signal-Generators-Based Single-Phase PLL Algorithms—A Survey .....	3932
..... Y. Han, M. Luo, X. Zhao, J. M. Guerrero, and L. Xu	
A Digital Hysteresis Current Controller for Three-Level Neutral-Point-Clamped Inverter With Mixed-Levels and Prediction-Based Sampling .....	3945
..... H. Yi, F. Zhuo, F. Wang, and Z. Wang	
$LLCL$ -Filtered Grid Converter With Improved Stability and Robustness .....	3958
..... M. Huang, X. Wang, P. C. Loh, and F. Blaabjerg	
Fast and Robust Single-Phase $DQ$ Current Controller for Smart Inverter Applications .....	3968
..... M. Ebrahimi, S. A. Khajehoddin, and M. Karimi-Ghartemani	

---

# Robustness Analysis and Experimental Validation of a Fault Detection and Isolation Method for the Modular Multilevel Converter

Shuai Shao, Alan J. Watson, *Member, IEEE*, Jon C. Clare, *Senior Member, IEEE*, and Pat W. Wheeler, *Senior Member, IEEE*

**Abstract**—This paper presents a fault detection and isolation (FDI) method for open-circuit faults of power semiconductor devices in a modular multilevel converter (MMC). The proposed FDI method is simple with only one sliding-mode observer (SMO) equation and requires no additional transducers. The method is based on an SMO for the circulating current in an MMC. An open-circuit fault of power semiconductor device is detected when the observed circulating current diverges from the measured one. A fault is located by employing an assumption-verification process. To improve the robustness of the proposed FDI method, a new technique based on the observer injection term is introduced to estimate the value of the uncertainties and disturbances; this estimated value can be used to compensate the uncertainties and disturbances. As a result, the proposed FDI scheme can detect and locate an open-circuit fault in a power semiconductor device while ignoring parameter uncertainties, measurement error, and other bounded disturbances. The FDI scheme has been implemented in a field-programmable gate array using fixed-point arithmetic and tested on a single-phase MMC prototype. Experimental results under different load conditions show that an open-circuit faulty power semiconductor device in an MMC can be detected and located in less than 50 ms.

**Index Terms**—Fault detection and isolation (FDI), modular multilevel converter (MMC), sliding-mode observer (SMO).

## I. INTRODUCTION

THE modular multilevel converter (MMC) is the state of the art in multilevel converters and is receiving great interest both from academia and industry. It has a number of desirable features such as modular configuration, low harmonic distortion, low-voltage stress on the semiconductor devices, high-voltage and high-power capability, and simple realization of redundancy [1]. In addition, the cells of an MMC are fed by capacitors and no multiphase transformers are required. A comprehensive introduction of the operation of the MMC is given in [2]. The review paper [3] summarizes the latest achievements regarding the MMC in terms of modeling, control, modulation, applications, and future trend.

Manuscript received October 8, 2014; revised March 27, 2015, January 19, 2015, and June 10, 2015; accepted July 22, 2015. Date of publication July 29, 2015; date of current version December 10, 2015. Recommended for publication by Associate Editor A. Perez.

The authors are with the Power Electronics, Machines and Control Group, School of Electrical and Electronic Engineering, The University of Nottingham, Nottingham NG7 2RD, U.K. (e-mail: eexs21@nottingham.ac.uk; Alan.watson@nottingham.ac.uk; Jon.Clare@nottingham.ac.uk; Pat.Wheeler@nottingham.ac.uk).

Color versions of one or more of the figures in this paper are available online at <http://ieeexplore.ieee.org>.

Digital Object Identifier 10.1109/TPEL.2015.2462717

Power semiconductor switches are among the most failure-prone components in a power converter and each of these devices is a potential failure point [4]. With large numbers of semiconductor devices, the possibility of fault occurrence is much larger than for normal two-level voltage-source converters (VSCs). Faults in power semiconductor devices cause a power converter operating far away from its setting point and this abnormal operation cannot be overcome by a feedback controller. If the faulty operation is allowed, other devices may be damaged and a shutdown of the plant may follow. Therefore, it is vital to detect and isolate these faults immediately after their occurrence.

Fault detection and isolation (FDI) deals with detecting anomalous situations [fault detection (FD)] and addressing their causes (fault isolation, FI) [5]. An FDI scheme can be implemented either by hardware method or analytical (software) method [5], [6]. Hardware FDI employs repeated components or additional sensors, and a fault can be obtained if the behavior of the process components is different from the redundant ones, or the additional sensors detect anomalous signals. It is straightforward and reliable but increases the cost, size, and hardware complexity of the plant. The basic idea of analytical FDI is to check the consistency between the actual system behavior and its estimated behavior [7]. The estimated behavior can be obtained either from a mathematical model of the system (for example, using observers) or an analysis of the historical data (for example, using data mining or neural networks). Although the algorithm is more sophisticated, the cost and hardware complexity of employing the analytical method is less than that for the hardware method. The application of the analytical FDI methods is boosted by the great advances of the computer technology in recent decades [6].

There are two types of faults seen in a fully controlled power semiconductor device: short-circuit fault (remains ON regardless of the gate signal) and open-circuit fault (remains OFF regardless of the gate signal). Any short-circuit fault needs to be detected within 10  $\mu$ s to save the semiconductor devices from destruction and to avoid a shoot-through fault with the complementary device [8]. A short circuit in an insulated-gate bipolar transistor (IGBT) is usually detected using a hardware circuit, often with additional sensors and associate circuits. These sensors and circuits are usually integrated in a gate driver to form an active/smart gate driver [9], [10]. The additional sensors and circuits add extra cost and size to the system. Furthermore, these active gate drivers can fail themselves due to their complexity and hence decrease the reliability of the power converter.

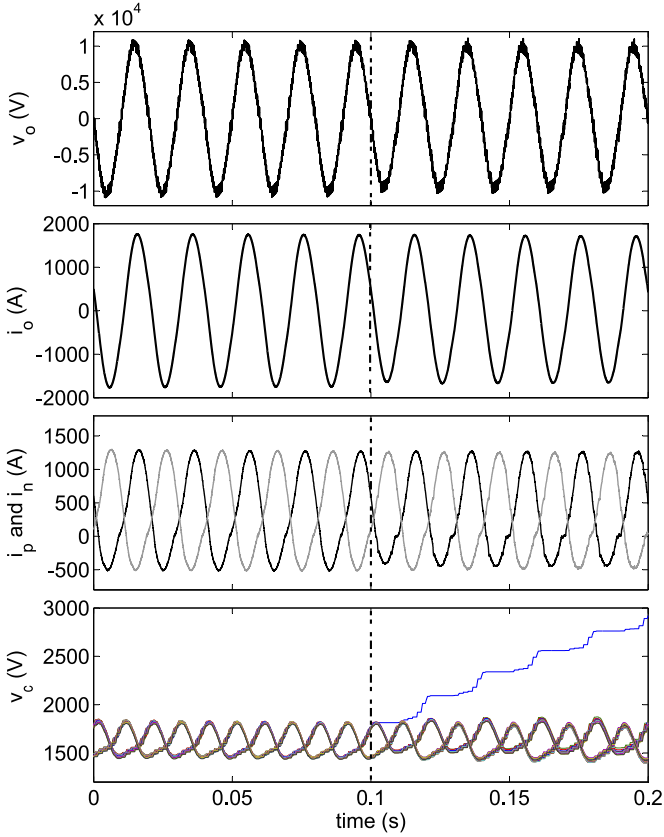


Fig. 1. Simulation results of an MMC with parameters same as an industrial 24-MW MMC and an open-circuit fault occurs at 0.1 s: from top to bottom, output voltage ( $v_o$ ), output current ( $i_o$ ), arm currents ( $i_p$  and  $i_n$ ), and capacitor voltages ( $v_c$ ).

This paper deals with detection and isolation of an open-circuit faulty switch in an MMC. The typical characteristics of an MMC in the event of an open-circuit fault in a power device is shown in Fig. 1, where the parameters are same as an industrial 24-MW MMC [11] and an open-circuit fault occurred at 0.1 s. Only one of the phases is considered. It can be seen that an open-circuit fault is not fatal immediately to an MMC; however, the fault needs to be detected and removed within 0.1 s to avoid secondary damages on other devices. The cause of an open-circuit fault can be various: lifting/fusing of bonding wires, a driver failure, or a communication problem between the controller and driver. The gate driver is recognized as the third most failure prone components according to an industry-based survey [12]. The simplest detection method is to use an active gate driver as mentioned previously. Analytical redundancy can be used to detect an open-circuit fault as this type of fault is not fatal immediately and can be tolerated by the power converter for some time [13]. Several analytical FDI methods based on the analysis of the output voltage waveform are reported. In [14], a faulty cell in a flying capacitor converter is detected and localized by analyzing the switching frequency of the output phase voltage. This technique has also been applied to a cascaded H-bridge [15] where an open- or short-circuit fault can be detected. In [16], the characteristics of the output phase voltage are analyzed in the time domain, and the occurrence of a fault is

detected by the degradation of the output voltage, while the fault is located by comparing the output phase voltage with all the possible phase fault voltages. In [17], an artificial intelligence FDI algorithm is proposed, where the historical data of the output phase voltages both in normal and faulty conditions are used to train a neural network. Survey [18] has presented a comprehensive review of the reliability of power electronics systems including methodologies of assessing reliability, methods to detect and locate faults as well as fault tolerate operation. Survey [19] has summarized the recent fault tolerance techniques for three-phase VSCs.

A sliding-mode observer (SMO)-based FDI technique for an MMC was proposed in [20] and [21], where a faulty power semiconductor device can be detected and located within 100 ms. The work presented in this paper is an improved method. This method is simpler using only one SMO equation and can detect and locate an open-circuit fault in less than 50 ms. Furthermore, a technique is proposed to compensate for any parameter uncertainties, measurement errors, and other bounded disturbances. The resultant FDI scheme can detect an open-circuit faulty power semiconductor device while rejecting any uncertainties and disturbances. The practical implementation of the SMO-based FDI scheme in a field-programmable gate array (FPGA) is also discussed in this paper and the experimental results at different load conditions are presented.

## II. SLIDING-MODE OBSERVER

### A. Introduction

An observer is a mathematical replica of a system to estimate its internal states, driven by the input of the system and a signal representing the discrepancy between the estimated and actual states [22]. In the earliest observers such as the Luenberger observer, the differences between the estimated outputs and the actual outputs of the plant are fed back to the observer linearly, and the estimated states cannot converge to the measured states in the presence of a disturbance [22], [23]. The SMO employs a high-gain switching function of the discrepancy between the estimated and actual outputs to force the estimated states to the actual states asymptotically.

A first-order system (1) is used in this paper

$$\dot{x} = ax + u. \quad (1)$$

An SMO for (1) is introduced

$$\dot{\hat{x}} = a\hat{x} + bu + L\text{sgn}(x - \hat{x}) \quad (2)$$

$$\text{sgn}(x) = \begin{cases} 1, & x > 0 \\ 0, & x = 0 \\ -1, & x < 0 \end{cases} \quad (3)$$

where  $\hat{x}$  donates the estimated/observed state of  $x$  and  $L$  denotes the observer gains designed to drive  $\hat{x} \rightarrow x$  in finite time. Subtracting (2) from (1) yields the dynamic error between the observed and measured states

$$\dot{\tilde{x}} = a\tilde{x} - L\text{sgn}(\tilde{x}), \tilde{x} \triangleq x - \hat{x}. \quad (4)$$



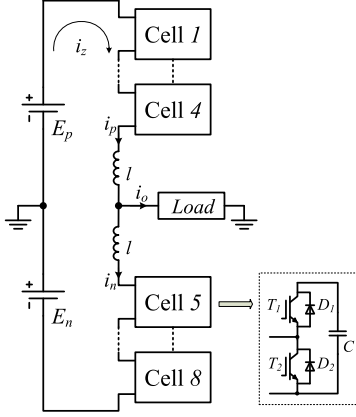


Fig. 2. Single-phase eight-cell MMC converter used for simulation.

TABLE I  
CIRCUIT PARAMETERS USED IN THE SIMULATION

DC voltage	$E_p + E_n$	6000 V
Average circulating current	$I_z$	120 A
Nominal voltage of the cell capacitors	$V_c$	1500 V
Capacitance of cell capacitors	$C$	4 mF
Inductance of the arm inductors	$l$	3 mH
Load		5 $\Omega$ , 4 mH

Choosing  $L > |a\tilde{x}|$ , we obtain

$$\tilde{x}\dot{\tilde{x}} = \tilde{x}(a\tilde{x} - L\text{sgn}(\tilde{x})) = |\tilde{x}|(|a\tilde{x}| - L) < 0 \quad (5)$$

which will force  $\tilde{x}$  and  $\dot{\tilde{x}}$  to zero and keep zero thereafter, this motion along a line is the so-called *sliding mode* [24].

### B. SMO for an MMC

An SMO can be built for an MMC based on (2). In this paper a single-phase eight-cell MMC is considered; nevertheless, the method is versatile and can be used for MMC with hundreds of cells.

The circuit diagram and parameters of the MMC used for the analysis and simulation are presented in Fig. 2 and Table I, respectively.  $T_1$  and  $T_2$  in Fig. 2 represent the upper and lower power semiconductor devices in a cell.

According to the Kirchhoff's voltage law, we obtain the following equation for the MMC (see Fig. 2):

$$l\frac{di_p}{dt} + l\frac{di_n}{dt} = -\sum_{i=1}^8 S_i v_{ci} + E_p + E_n \quad (6)$$

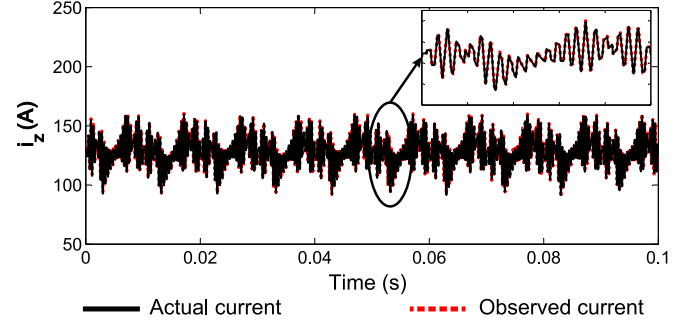
where  $i_p$  and  $i_n$  are the upper and lower arm currents,  $l$  is the inductance of arm inductors,  $E_p$  and  $E_n$  are the dc voltages, and  $v_{ci}$  and  $S_i$  are the capacitor voltage and switching state of the cell  $i$ , respectively.  $S_i$  is defined in Table II, where  $g_1$  and  $g_2$  are the gate signals for the upper and lower switch in a cell.

Since the circulating current of the MMC converter is  $i_z = (i_p + i_n)/2$  [25], (6) can be rewritten as

$$2l\frac{di_z}{dt} = -\sum_{i=1}^8 S_i v_{ci} + E_p + E_n. \quad (7)$$

TABLE II  
SWITCHING STATE  $S$  IN NORMAL CONDITIONS

$S$	Driving signals
1	$g_1 = 1, g_2 = 0$
0	$g_1 = 0, g_2 = 1$

Fig. 3. Simulation waveforms of  $i_z$  and  $\hat{i}_z$  when the MMC is fault free.

Based on (2) and (7), an SMO can be obtained for the MMC

$$\frac{d\hat{i}_z}{dt} = -\frac{1}{2l} \left( \sum_{i=1}^8 S_i v_{ci} - E_p - E_n \right) + L\text{sat} \left( i_z - \hat{i}_z \right). \quad (8)$$

It is noted that a saturation function  $\text{sat}(x)$  (9) is utilized instead of  $\text{sgn}(x)$  for less chattering of the observed states according to [26]

$$\text{sat}(x) = \begin{cases} 1, & x \geq h \\ x/h, & -h < x < h, h > 0 \\ -1, & x \leq -h \end{cases} \quad (9)$$

where  $h$  is a constant.

A simulation has been carried out in SIMULINK/PLECS to verify the SMO (8). The parameters of the MMC are listed in Table I and the observer gain  $L$  is  $6 \times 10^4$  and  $h = 1$ . Fig. 3 shows the simulation results where it can be seen that  $\hat{i}_z$  follows  $i_z$  closely.

## III. FAULT DETECTION AND ISOLATION USING SMO

### A. Mathematical Basis

The *FD* is first considered and a fault is added to the first-order system

$$\dot{x} = ax + bu + kf \quad (10)$$

where  $f$  represents the value of the fault and  $k$  the corresponding coefficients. It is noted that  $f$  is often a very large value and cannot be overcome by the feedback control.

The difference between the observed and measured states can be obtained by subtracting (10) from (2)

$$\dot{\tilde{x}} = a\tilde{x} + kf - L\text{sgn}(\tilde{x}). \quad (11)$$

If we choose

$$L < |kf| \quad (12)$$

However, this method is not suitable for the detection and isolation of a short-circuit faulty device due to the very fast response requirement (10  $\mu$ s). It is suggested that the proposed method works together with the hardware detection methods (for short-circuit fault) to achieve a more reliable MMC.

To improve the robustness of the FDI method, a technique is proposed to estimate parameter uncertainties, measurement errors, and other bounded disturbances, and the estimated value is used to compensate for the influence of the uncertainties and disturbances. As a result, the proposed technique can detect and locate an open-circuit faulty power semiconductor device while ignoring the parameter uncertainties, measurement noise, or other disturbances.

The FDI algorithm has been implemented in an FPGA using fixed-point arithmetic and has been tested on an experimental scaled-down, single-phase, eight-cell MMC converter. Experimental results have verified the analysis and simulation results. According to the experimental results, it is possible to use a smaller threshold value to detect and locate an open-circuit fault in less than 20 ms.

This FDI method can be applied to other converters with modular topologies employing similar analysis and principles. Furthermore, it is possible to apply this method for the detection and isolation of multiple open-circuit faults in an MMC, although it will take longer to find the faults as there are many possible fault scenarios to be assumed.

#### ACKNOWLEDGMENT

The authors would like to thank Prof. G. Asher from the University of Nottingham and Dr. C. Oates from Alstom Grid for their constructive suggestions regarding this work.

#### REFERENCES

- [1] M. Glinka and R. Marquardt, "A new ac/ac multilevel converter family," *IEEE Trans. Ind. Electron.*, vol. 52, no. 3, pp. 662–669, Jun. 2005.
- [2] G. Adam, O. Anaya-Lara, G. Burt, D. Telford, B. Williams, and J. McDonald, "Modular multilevel inverter: Pulse width modulation and capacitor balancing technique," *IET Power Electron.*, vol. 3, no. 5, pp. 702–715, Sep. 2010.
- [3] M. Perez, S. Bernet, J. Rodríguez, S. Kouro, and R. Lizana, "Circuit topologies, modelling, control schemes and applications of modular multilevel converters," *IEEE Trans. Power Electron.*, vol. 30, no. 1, pp. 4–17, Jan. 2015.
- [4] F. Richardeau and T. Pham, "Reliability calculation of multilevel converters: Theory and applications," *IEEE Trans. Ind.*, vol. 60, no. 10, pp. 4225–4233, Oct. 2013.
- [5] R. Patton, R. Clark, and P. Frank, *Fault Diagnosis in Dynamic Systems: Theory and Applications* (ser. Prentice-Hall international series in systems and control engineering). New York, NY, USA: Prentice-Hall, 1989.
- [6] F. Caccavale and L. Villani, *Fault Diagnosis and Fault Tolerance for Mechatronic Systems: Recent Advances* (ser. Engineering online library). New York, NY, USA: Springer, 2003.
- [7] M. Kinnaert, "Fault diagnosis based on analytical models for linear and nonlinear systems—A tutorial," in *Proc. 15th Int. Workshop Principles Diagnosis*, 2003, pp. 37–50.
- [8] R. Chokhawala, J. Catt, and L. Kiraly, "A discussion on IGBT short-circuit behavior and fault protection schemes," *IEEE Trans. Ind. Appl.*, vol. 31, no. 2, pp. 256–263, Mar. 1995.
- [9] Z. Wang, X. Shi, L. Tolbert, F. Wang, and B. Blalock, "A di/dt feedback-based active gate driver for smart switching and fast overcurrent protection of IGBT modules," *IEEE Trans. Power Electron.*, vol. 29, no. 7, pp. 3720–3732, Jul. 2014.
- [10] L. Chen, F. Peng, and D. Cao, "A smart gate drive with self-diagnosis for power MOSFETs and IGBTs," in *Proc. 23rd Annu. IEEE Appl. Power Electron. Conf. Expo.*, Feb. 2008, pp. 1602–1607.
- [11] C. Davidson, A. Lancaster, A. Totterdell, and C. Oates, "A 24 mW level voltage source converter demonstrator to evaluate different converter topologies," in *Proc. Cigre*, 2012, pp. 0–9.
- [12] S. Yang, A. Bryant, P. Mawby, D. Xiang, L. Ran, and P. Tavner, "An industry-based survey of reliability in power electronic converters," *IEEE Trans. Ind. Appl.*, vol. 47, no. 3, pp. 1441–1451, May 2011.
- [13] R. Wu, F. Blaabjerg, H. Wang, M. Liserre, and F. Iannuzzo, "Catastrophic failure and fault-tolerant design of IGBT power electronic converters—An overview," in *Proc. 39th Annu. Conf. IEEE Ind. Electron. Soc.*, Nov. 2013, pp. 507–513.
- [14] F. Richardeau, P. Baudesson, and T. Meynard, "Failures-tolerance and remedial strategies of a PWM multicell inverter," *IEEE Trans. Power Electron.*, vol. 17, no. 6, pp. 905–912, Nov. 2002.
- [15] P. Lezana, R. Aguilar, and J. Rodriguez, "Fault detection on multicell converter based on output voltage frequency analysis," *IEEE Trans. Ind. Electron.*, vol. 56, no. 6, pp. 2275–2283, Jun. 2009.
- [16] A. Yazdani, H. Sepahvand, M. Crow, and M. Ferdowsi, "Fault detection and mitigation in multilevel converter STATCOMs," *IEEE Trans. Ind. Electron.*, vol. 58, no. 4, pp. 1307–1315, Apr. 2011.
- [17] S. Khomfoi and L. Tolbert, "Fault diagnosis and reconfiguration for multilevel inverter drive using ai-based techniques," *IEEE Trans. Ind. Electron.*, vol. 54, no. 6, pp. 2954–2968, Dec. 2007.
- [18] Y. Song and B. Wang, "Survey on reliability of power electronic systems," *IEEE Trans. Power Electron.*, vol. 28, no. 1, pp. 591–604, Jan. 2013.
- [19] B. MIRAFZAL, "Survey of fault-tolerance techniques for three-phase voltage source inverters," *IEEE Trans. Ind. Electron.*, vol. 61, no. 10, pp. 5192–5202, Oct. 2014.
- [20] S. Shao, P. Wheeler, J. Clare, and A. Watson, "Fault detection for modular multilevel converters based on sliding mode observer," *IEEE Trans. Power Electron.*, vol. 28, no. 11, pp. 4867–4872, 2013.
- [21] S. Shao, P. Wheeler, J. Clare, and A. Watson, "Open-circuit fault detection and isolation for modular multilevel converter based on sliding mode observer," in *Proc. 15th Eur. Conf. Power Electron. Appl.*, 2013, pp. 1–9.
- [22] Y. Shtessel, C. Edwards, L. Fridman, and A. Levant, *Sliding Mode Control and Observation* (ser. Control Engineering). New York, NY, USA: Springer, 2013.
- [23] V. Utkin, J. Guldner, and J. Shi, *Sliding Mode Control in Electro-Mechanical Systems* (ser. Automation and Control Engineering). Boca Raton, FL, USA: CRC Press, 2009.
- [24] V. Utkin, "Variable structure systems with sliding modes," *IEEE Trans. Autom. Control.*, vol. 22, no. 2, pp. 212–222, Apr. 1977.
- [25] M. Vasiladotiss, "Analysis, implementation and experimental evaluation of control systems for a modular multilevel converter," Master's thesis, Royal Inst. Technol., Stockholm, Sweden, 2009.
- [26] M. Almaleki, P. Wheeler, and J. Clare, "Sliding mode observer design for universal flexible power management (Uniflex-PM) structure," in *Proc. 34th Annu. Conf. IEEE Ind. Electron.*, Nov. 2008, pp. 3321–3326.
- [27] K. Ilves, S. Norrga, L. Harnefors, and H.-P. Nee, "On energy storage requirements in modular multilevel converters," *IEEE Trans. Power Electron.*, vol. 29, no. 1, pp. 77–88, Jan. 2014.
- [28] M. Hagiwara and H. Akagi, "Control and experiment of pulsewidth-modulated modular multilevel converters," *IEEE Trans. Power Electron.*, vol. 24, no. 7, pp. 1737–1746, Jul. 2009.



**Shuai Shao** received the B.Eng. degree from Zhejiang University, Hangzhou, China, in 2010, and the Ph.D. degree in electrical engineering for his work on fault detection for multilevel converter from the University of Nottingham, Nottingham, U.K., in 2015.

His research interests include fault detection, multilevel converters, and VSC-HVDC.



**Alan J. Watson** (S'03–M'08) received the M.Eng. (Hons.) degree in electronic engineering from the University of Nottingham, Nottingham, U.K., in 2004, and the Ph.D. degree in power electronics, also from the University of Nottingham.

In 2008, he became a Research Fellow in the Power Electronics Machines and Control Group, working on the UNIFLEX project (<http://www.eee.nott.ac.uk/uniflex/>). Since 2008, he has worked on several projects in the area of high-power electronics including high-power resonant

converters, high-voltage power supplies, and multilevel converters for grid-connected applications such as HVDC and FACTS. In 2012, he was promoted to a Senior Research Fellow before becoming a Lecturer in high-power electronics in 2013. His research interests include the development and control of advanced high-power conversion topologies for industrial applications, future energy networks, and VSC-HVDC.



**Pat W. Wheeler** (SM'11) received the B.Eng. (Hons.) degree in, 1990, and the Ph.D. degree in electrical engineering for his work on matrix converters, in 1994, both from the University of Bristol, Bristol, U.K.

In 1993, he moved to the University of Nottingham, Nottingham, U.K., and worked as a Research Assistant in the Department of Electrical and Electronic Engineering. In 1996, he became a Lecturer in the Power Electronics, Machines and Control Group, The University of Nottingham. Since January 2008,

he has been a Full Professor in the same research group. He has published 400 academic publications in leading international conferences and journals.

Dr. Wheeler is a Member at Large and Distinguished Lecturer of the IEEE Power Electronics Society.



**Jon C. Clare** (M'90–SM'04) was born in Bristol, U.K., in 1957. He received the B.Sc. and Ph.D. degrees in electrical engineering from the University of Bristol, Bristol.

From 1984 to 1990, he was a Research Assistant and Lecturer with the University of Bristol, where he was involved in teaching and research on power electronic systems. Since 1990, he has been with the Power Electronics, Machines and Control Group, The University of Nottingham, Nottingham, U.K., where he is currently a Professor of power electronics. His

research interests include power-electronic converters and modulation strategies, variable-speed-drive systems, and electromagnetic compatibility.



2014

IEEE ENERGY CONVERSION CONGRESS & EXPO | PITTSBURGH, PA, USA | SEPTEMBER 14-18, 2014

SPONSORED BY THE IEEE POWER ELECTRONICS  
AND INDUSTRY APPLICATIONS SOCIETIES



# PROCEEDINGS

IEEE ENERGY CONVERSION CONGRESS & EXPOSITION®

Welcome

Meeting Supporters

Schedule at a Glance

Leadership

Table of Contents

Author Index

Tutorials

2015 Call for Papers

Copyright

Search

Help

IEEE Catalog Number: CFP14ECD-USB • ISBN: 978-1-4 799-5698-2 • Copyright and Reprint Permission: Abstracting is permitted with credit to the source. Libraries are permitted to photocopy beyond the limit of U.S. copyright law for private use of patrons those articles in this volume that carry a code at the bottom of the first page, provided the per-copy fee indicated in the code is paid through Copyright Clearance Center, 222 Rosewood Drive, Danvers, MA 01923. For other copying, reprint or republication permission, write to IEEE Copyrights Manager, IEEE Operations Center, 445 Hoes Lane, Piscataway, NJ 08854. All rights reserved. © Copyright 2014 by IEEE.

Digital media support, contact The Printing House, Inc. at +1-608-873-4500. For more information, please see the "Copyright" page.



**Shafiei, Navid**

High Power LLC Battery Charger: Wide Regulation using Phase-Shift for Recovery Mode

**Shan, Zhenyu**

Resonant Augmentation Circuits for a Buck Converter Achieving Minimum-Time Voltage Recovery from Load Transients

**Shang, Jianing**

An Iteration Method for Determining Critical Stable Regions of Shunt Regulator with Multistage Hysteresis Control and its Complex Behaviors

**Shao, Shuai**

Detection and Isolation of Multiple Faults in a Modular Multilevel Converter based on a Sliding Mode Observer

**Shapoury, Alireza**

Analysis and Development of an Axial Flux Magnetic Gear

**Sharma, Yogesh**

Evaluation of Commercially Available SiC Devices and Packaging Materials for Operation Up to 350°C

**She, Hongwei**

Dual Sequence Current Controller without Current Sequence Decomposition Implemented on DSRF for Unbalanced Grid Voltage Conditions

**She, Shuojie**

Thermal Analysis and Improvement of Cascode GaN HEMT in Stack-Die Structure

**She, Xu**

Decentralized Architecture and Control of Photovoltaic Generation System based on Cascaded AC Module Integrated Converter

A High Performance Controller for a Single Phase Cascaded Multilevel Photovoltaic System

**Shea, Adam**

Hardware Integration for an Integrated Modular Motor Drive Including Distributed Control

**Shek, Jonathan K.H.**

The Measurement and Indexing of Unbalanced Magnetic Pull in Electrical Machines

**Shen, Dan**

A Hybrid Wind-Solar-Storage Energy Generation System Configuration and Control

# Detection and Isolation of Multiple Faults in a Modular Multilevel Converter based on a Sliding Mode Observer

Shuai Shao, Jon C. Clare, Alan J. Watson and Patrick W. Wheeler  
PEMC, School of Electrical and Electronic Engineering,  
University of Nottingham,  
Nottingham, UK NG7 2RD  
Email: eexss21@nottingham.ac.uk

**Abstract**—This paper proposes a technique able to detect and isolate multiple open-circuit faults of power switches in an MMC. Based on a sliding mode observer (SMO), the basic idea of this FDI method is to compare the observed states with the measured states. The fault occurrence is detected when the difference between the observed and measured arm current is larger than a threshold value; while a cell is identified as faulty if the difference between the observed and measured capacitor voltage is larger than a threshold value. The implementation is simple and requires no additional sensors. Simulation results demonstrate that open-circuit faults occurring simultaneously on four different cells in an MMC can be detected and isolated within 200ms.

## I. INTRODUCTION

One of the most important applications of the modular multilevel converter (MMC) is high-voltage direct current (HVDC) transmission [1], [2]. The first commercial HVDC project using MMC, the Trans Bay Cable project, went in service in 2010 transmitting up to 400MW and a few other similar projects with power rating between 576MW and 1000MW have been reported [3]. With hundreds of cells per converter arm in these practical MMC systems, the possibility of a fault occurrence in the semiconductor switching devices increases significantly compared with two- or three-level voltage source converters.

For a power switch, there are two types of faults: short-circuit fault (remains ON regardless of the gate signal) and open-circuit fault (remains OFF regardless of the gate signal). Short-circuit faults are often detected by a de-saturation detector integrated in the gate driver. This paper deals with open-circuit faults on power switches. The causes of an open-circuit fault of a semiconductor switching device can be various: an open-circuit fault of the device itself (i.e. lifting/fusing of bond wires), failure of the driver or communication problems between the controller and driver. In the presence of an open-circuit fault of a device in an MMC, the capacitor voltage of a cell cannot be controlled. This can lead to possible damage of capacitors and other switches, and a shut-down of the plant may follow. Therefore, it is vital to detect and isolate these faults immediately after their occurrence.

Fault detection and isolation (FDI) deals with detecting anomalous situations (fault detection) and addressing their

causes (fault isolation) [4]. An FDI scheme can be implemented either using hardware redundancy or analytical (software) redundancy [4], [5]. Hardware redundancy employs repeated components or additional sensors, and a fault can be obtained if the behaviours of the process components are different from the redundant ones, or the additional sensors detect anomalous signals. Hardware redundancy is straightforward and reliable but increases the cost and complexity in the case of an MMC plant. The basic idea of analytical redundancy is to check the consistency between the actual system behaviour and its estimated behaviour [6]. The estimated behaviour can either be obtained from a mathematical model of the system (for example observers) or analysis of the historical data (for example using data mining or neural networks). Although it requires a rather sophisticated algorithm, the cost and hardware complexity of an analytical solution is less than a hardware redundancy solution.

For the FDI of a multilevel converter, the simplest way is to add additional current and voltage transducers to sense the current through and voltage across each power switch, this is however very costly. In [7], the characteristics of the gate signal are analysed to detect an open-circuit fault or short-circuit fault of a switch. The phase voltage is also used to detect and locate a fault: in [8], [9], the phase voltage is analysed in the frequency domain, while in [10] the phase voltage is analysed in the time domain.

In [11], [12], a single open-circuit fault has been detected and isolated using a sliding mode observer (SMO). This paper presents a method using an SMO to detect and isolate faulty cells when there are multiple faults occurring simultaneously in power switches. This method uses the inputs which are already available in the control system and requires no additional sensors. A detailed simulation study has shown that the potential to locate one or more open-circuit faults within 200ms.

## II. SLIDING MODE OBSERVER

An observer is a contrivance designed from a real system, generally in the same mathematical form as the original system, so as to estimate its internal state [13]. An SMO uses a high gain feedback in the observer vector (normally in the form of a high frequency switching function, for example the saturation function of an observed-measured error, as (3)

# Detection and Isolation of Multiple Faults in a Modular Multilevel Converter based on a Sliding Mode Observer

Shuai Shao, Jon C. Clare, Alan J. Watson and Patrick W. Wheeler  
PEMC, School of Electrical and Electronic Engineering,  
University of Nottingham,  
Nottingham, UK NG7 2RD  
Email: eexss21@nottingham.ac.uk

**Abstract**—This paper proposes a technique able to detect and isolate multiple open-circuit faults of power switches in an MMC. Based on a sliding mode observer (SMO), the basic idea of this FDI method is to compare the observed states with the measured states. The fault occurrence is detected when the difference between the observed and measured arm current is larger than a threshold value; while a cell is identified as faulty if the difference between the observed and measured capacitor voltage is larger than a threshold value. The implementation is simple and requires no additional sensors. Simulation results demonstrate that open-circuit faults occurring simultaneously on four different cells in an MMC can be detected and isolated within 200ms.

## I. INTRODUCTION

One of the most important applications of the modular multilevel converter (MMC) is high-voltage direct current (HVDC) transmission [1], [2]. The first commercial HVDC project using MMC, the Trans Bay Cable project, went in service in 2010 transmitting up to 400MW and a few other similar projects with power rating between 576MW and 1000MW have been reported [3]. With hundreds of cells per converter arm in these practical MMC systems, the possibility of a fault occurrence in the semiconductor switching devices increases significantly compared with two- or three-level voltage source converters.

For a power switch, there are two types of faults: short-circuit fault (remains ON regardless of the gate signal) and open-circuit fault (remains OFF regardless of the gate signal). Short-circuit faults are often detected by a de-saturation detector integrated in the gate driver. This paper deals with open-circuit faults on power switches. The causes of an open-circuit fault of a semiconductor switching device can be various: an open-circuit fault of the device itself (i.e. lifting/fusing of bond wires), failure of the driver or communication problems between the controller and driver. In the presence of an open-circuit fault of a device in an MMC, the capacitor voltage of a cell cannot be controlled. This can lead to possible damage of capacitors and other switches, and a shut-down of the plant may follow. Therefore, it is vital to detect and isolate these faults immediately after their occurrence.

Fault detection and isolation (FDI) deals with detecting anomalous situations (fault detection) and addressing their

causes (fault isolation) [4]. An FDI scheme can be implemented either using hardware redundancy or analytical (software) redundancy [4], [5]. Hardware redundancy employs repeated components or additional sensors, and a fault can be obtained if the behaviours of the process components are different from the redundant ones, or the additional sensors detect anomalous signals. Hardware redundancy is straightforward and reliable but increases the cost and complexity in the case of an MMC plant. The basic idea of analytical redundancy is to check the consistency between the actual system behaviour and its estimated behaviour [6]. The estimated behaviour can either be obtained from a mathematical model of the system (for example observers) or analysis of the historical data (for example using data mining or neural networks). Although it requires a rather sophisticated algorithm, the cost and hardware complexity of an analytical solution is less than a hardware redundancy solution.

For the FDI of a multilevel converter, the simplest way is to add additional current and voltage transducers to sense the current through and voltage across each power switch, this is however very costly. In [7], the characteristics of the gate signal are analysed to detect an open-circuit fault or short-circuit fault of a switch. The phase voltage is also used to detect and locate a fault: in [8], [9], the phase voltage is analysed in the frequency domain, while in [10] the phase voltage is analysed in the time domain.

In [11], [12], a single open-circuit fault has been detected and isolated using a sliding mode observer (SMO). This paper presents a method using an SMO to detect and isolate faulty cells when there are multiple faults occurring simultaneously in power switches. This method uses the inputs which are already available in the control system and requires no additional sensors. A detailed simulation study has shown that the potential to locate one or more open-circuit faults within 200ms.

## II. SLIDING MODE OBSERVER

An observer is a contrivance designed from a real system, generally in the same mathematical form as the original system, so as to estimate its internal state [13]. An SMO uses a high gain feedback in the observer vector (normally in the form of a high frequency switching function, for example the saturation function of an observed-measured error, as (3)

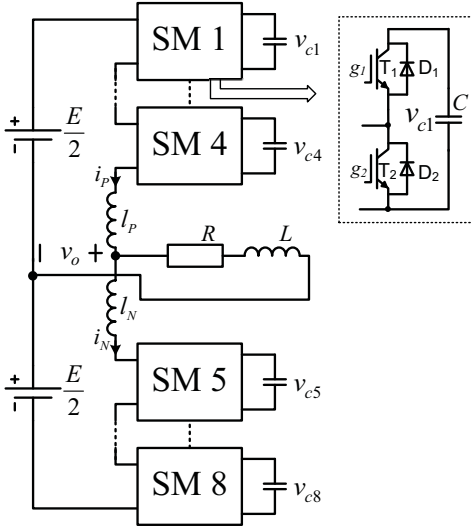


Fig. 1. An eight-cell single phase MMC.

TABLE I. SWITCHING STATE  $S$  OF A SUBMODULE

$S$	Driving signals
1	$g_1 = 1, g_2 = 0$
0	$g_1 = 0, g_2 = 1$

and (4) present) to force the observed output to converge to a measured output [13][14]. The SMO offers desirable features such as robustness to parameter uncertainty and insensitivity to measurement noise [13], [15], [14].

Fig. 1 is an eight-cell single phase MMC. According to the Kirchhoffs voltage law (KVL), its characteristics can be described by

$$\begin{cases} l_P \dot{i}_P + l_N \dot{i}_N = -\sum_{j=1}^8 S_j v_{cj} + E \\ C \dot{v}_{cj} = S_j \cdot i_P \quad (j = 1, 2, 3, 4) \\ C \dot{v}_{cj} = S_j \cdot i_N \quad (j = 5, 6, 7, 8) \end{cases} \quad (1)$$

where  $i_P$  and  $i_N$  are the upper and lower arm currents,  $l_P$  and  $l_N$  are the inductances of the upper and lower arm inductors,  $E$  is the DC voltage,  $v_{c1}, v_{c2}, \dots, v_{c8}$  are the capacitor voltages of Cell 1 to 8,  $C$  is the capacitance of the capacitors of cells and  $S_j$  is the switching state of the SM  $j$  and it is defined in Table I.

If we let  $i_a = k \cdot i_P + i_N$ , where  $k = l_P/l_N$ , the first line of (1) can be rewritten as

$$\dot{i}_a = -\frac{1}{l_N} \left( \sum_{j=1}^8 S_j v_{cj} - E \right). \quad (2)$$

An SMO can be constructed to observe the arm current based on (2):

$$\frac{d\hat{i}_a}{dt} = -\frac{1}{l_N} \left( \sum_{j=1}^8 S_j v_{cj} - E \right) + L_1 \text{sat} \left( i_a - \hat{i}_a \right). \quad (3)$$

where  $\hat{i}_a$  donates the observed current,  $L_1$  is the observer gain and  $\text{sat}(x)$  is the saturation function define as

$$\text{sat}(x) = \begin{cases} 1 & x \geq h \\ x/h & -h < x < h, \quad h > 0 \\ -1 & x \leq -h \end{cases} \quad (4)$$

When the MMC converter works normally,  $\hat{i}_a$  converges to  $i_a$ . Indeed, subtracting (3) from (2) yields

$$\dot{\tilde{i}}_a = -L_1 \text{sat}(\tilde{i}_a), \tilde{i}_a \triangleq i_a - \hat{i}_a. \quad (5)$$

Choosing  $L_1 > 0$ , we obtain  $\tilde{i}_a \dot{\tilde{i}}_a = -L_1 \tilde{i}_a \text{sat}(\tilde{i}_a) < 0$ , which will force  $\hat{i}_a \rightarrow i_a$  in a finite time. A larger number is often chosen for  $L_1$  to overcome the influence of the disturbances and uncertainties.

A simulation is carried out in SIMULINK/PLECS with circuit parameters in Table II. Fig. 2 shows the simulated results. In the upper part of Fig. 2, the MMC converter operates normally and the observed current  $\hat{i}_a$  follows the measured current  $i_a$  closely. In the bottom part of Fig. 2, an open-circuit fault occurs in the switches of both Cell 1 and 6, and  $\hat{i}_a$  diverges from  $i_a$  significantly. This phenomenon, which will be detailed in the following sections, can be used for fault detection and isolation.

TABLE II. CIRCUIT PARAMETERS USED IN THE SIMULATION.

DC voltage	$E$	12800V
DC capacitor voltage	$V_c$	3200V
Upper arm inductor	$l_P$	3.3mL
Lower arm inductor	$l_N$	3mL
Cell capacitors	$C$	2.2mF
Observer gain	$L_1$	320,000
Observer gain	$L_2$	10,000
Threshold value for FD	$I_{th}$	300
Threshold value for FI	$V_{th}$	400

### III. FAULT DETECTION AND ISOLATION ALGORITHM FOR MMC

The FDI algorithm has two parts: fault detection (FD) and fault isolation (FI). The FD mode monitors whether the MMC is healthy and the FI mode is used to locate the faulty cells and bypass them.

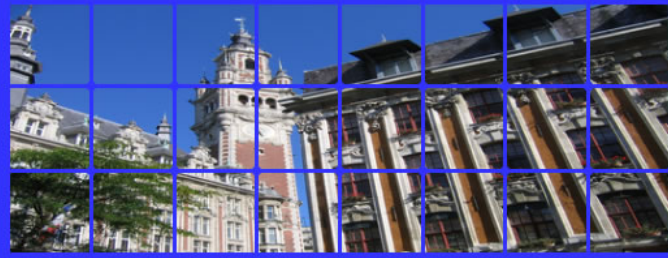
#### A. Fault Detection (FD)

As we noticed from Fig. 2 in Section II, the observed current diverges from the measured current after the occurrence of the open-circuit faults. In general faults at any cell will be reflected in  $\hat{i}_a$ , and under faulty conditions (2) becomes

$$\dot{i}_a = -\frac{1}{l_N} \left( \sum_{j=1}^8 S_j v_{cj} - E \right) + f_1. \quad (6)$$

where  $f_1$  donates the value of a fault, it is a large value and cannot be eliminated by feedback control and thus it needs

EPE'13 ECCE Europe  
15th European Conference  
on Power Electronics  
and Applications  
3-5 September 2013  
Lille, France



[\[Home\]](#) [Objectives](#) - [Topics](#) [Organization](#) [Venue](#) [Sponsors](#) [Exhibitors](#) [Future Events](#) [Programme](#) [Papers](#) [Contact](#) [Credits](#)

[3 September 2013](#)

[4 September 2013](#)

[5 September 2013](#)

Programme

[3 September 2013](#) [4 September 2013](#) [5 September 2013](#)

**3 September 2013**

*Click on the titles to open the pdf files.*

08:35, Keynote, Opening address

- [Day 1 - Opening Address: The strategic role of grids](#)

08:55, Keynote, Keynote 1: Power electronics enabling the grid of the future

- [Day 1 - Keynote 1a - Grids: Smart Grids : large scale experimentation in Vendée and future markets for power electronics](#)
- [Day 1 - Keynote 1b - Grids: First return on experience on Smart Grids Demonstrations : emergence of new System of systems architectures](#)

09:25, Keynote, Keynote 2: Power Electronics for Aerospace

- [Day 1 - Keynote 2 - Aeronautics: The era of the electrical aircraft](#)

10:30, Lecture, LS1a: Industrial session: Power Electronics for the Grid

- [A roadmap to the development of the Supergrid](#)
- [Cable technologies for HVDC connections and interconnections](#)
- [Cigre and Trends in Power Electronics for the Grid](#)
- [Medgrid - An industrial initiative for the development of interconnections between the Mediterranean power grids](#)

10:30, Lecture, LS1b: Industrial Session: The Aerospace Industry

- [Effect of the lightning on more electric and more composite aircrafts](#)
- [Electric Taxi for Airport traffic](#)
- [FP7-project ACTUATION 2015: objective and progress](#)
- [Full electric Trust Vector Control for space launcher applications](#)

10:30, Lecture, LS1c: Topic 2: Passive Components and Integrated Passive Components

- [Acoustic Noise in Inductive Power Components](#)
- [Analytical model for the thermal resistance of windings consisting of solid or litz wire](#)
- [Capacitors for High Temperature DC Link Applications in Automotive Traction Drives: Current Technology and Limitations](#)
- [Design and Optimization of Medium Frequency, Medium Voltage Transformers](#)

10:30, Lecture, LS1d: Topic 6: Converter Control, Current/Voltage Control (I)

- [Comparison of Linear and Predictive Control Employing Different Current Reference Strategies for Unbalance Voltage Sources](#)
- [Impact of Modulation Schemes on the Power Capability of High Power Converters with Low Pulse Ratios](#)
- [Self-commissioning Notch Filter for Active Damping in Three Phase LCL-filter Based Grid Converters](#)
- [Space-Vector-Modulated Three-level Z-source Hybrid Direct AC-AC Power Converter](#)

10:30, Lecture, LS1e: Topic 8: Measurement Methods and Techniques

- [ACCURATE SWITCHING ENERGY ESTIMATION OF WIDE BANDGAP DEVICES USED IN CONVERTERS FOR AIRCRAFT APPLICATIONS](#)
- [DC-bias current measurement in high power AC grids](#)
- [New applications in power electronics for highly integrated high-speed magnetoresistive current sensors](#)
- [Parallel Chamber Calorimetric Concept](#)

10:30, Lecture, LS1f: Topic 17: Power Factor Correction

- [A Voltage-Sensorless Interleaved Rectifier with PFC](#)
- [High Performance Direct Power Control of Three-Phase PWM Boost Rectifier under Different Supply Voltage Conditions](#)
- [New Unidirectional High-Efficiency Three-Level Single-Phase Bridgeless PFC Rectifier](#)
- [Single-Phase/-Stage NPC-Based Rectifier Integrating a Simple DCM PFC Technique](#)

10:30, Lecture, LS1g: Topic 12: Advanced Control and other High Performance Drive System Issues

- [Extended Straightforward Current Control for Permanent Magnet Synchronous Machines](#)



- [Model-based Voltage Phase Control for IPMSM with Equilibrium Point Search](#)
- [Robustness analysis of deadbeat, direct torque and flux control for IPMSM drives](#)
- [Space Vector Modulation technique for common mode current reduction in Multiphase AC drives](#)

12:00, Lecture, LS2a: Industrial Session Grids

- [Multilevel Modular Converter Design and optimization](#)
- [Power Electronics for Energy efficiency and Smart grid : Innovations and perspective](#)
- [Rand D opportunities for Supergrid issues : technological projects](#)
- [Wind Energy integration, an operator point of view](#)

12:00, Lecture, LS2b: Industrial Session: aerospace

- [Multi-Generator System Modelling Based on Dynamic Phasor Concept](#)
- [Optimizing Power Electronic for More Electrical Aircraft](#)
- [Power electronics and new power centres in more electric aircraft](#)
- [Protection of local High Voltage DC regenerative network on More Electric Aircraft](#)

12:00, Lecture, LS2c: Topic 2: Passive Components, System Integration & Packaging

- [Assessment of selected materials and assembly technologies for power electronics modules with the capability to operate at high temperatures](#)
- [Impact of Absolute Junction Temperature on Power Cycling Lifetime](#)
- [Multi-switch Si-chip structures and on-substrate packaging techniques for improving the electrical performance of power modules](#)
- [Real-time degradation monitoring and lifetime estimation of 3D integrated bond-wire-less double-sided cooled power switch technologies](#)

12:00, Lecture, LS2d: Topic 6: Converter Control, Current/Voltage Control (II)

- [Arm-current-based control of Modular Multilevel Converters](#)
- [Control Strategy with Variable Commutation Instants for MPC Based on Two Flying Capacitors Connected in Parallel](#)
- [Open-circuit Fault Detection and Isolation for Modular Multilevel Converter Based on Sliding Mode Observer](#)
- [Tolerance Band Modulation Methods for Modular Multilevel Converters](#)

12:00, Lecture, LS2e: Topic 8: Hardware-in-the-Loop Systems

- [Laboratory-based test bed of a three terminals DC networks using Power Hardware In the Loop](#)
- [Online estimation of IGBT junction temperature \( \$T\_j\$ \) using gate-emitter voltage \( \$V\_{ge}\$ \) at turn-off](#)
- [PHIL Simulation for Validating Power Management Strategies in All-electric Vehicles](#)
- [Review of state-of-the-art solver solutions for HIL simulation of power systems, power electronic and motor drives](#)

12:00, Lecture, LS2f: Topic 17: Electronic Ballasts and Solid State Lighting

- [A TRIAC Dimmable Driver Design for High Dimmer Compatibility in Low Power LED Lighting](#)
- [Designing the high voltage transformer of power supplies for DBD: windings arrangement to reduce the parasitic capacitive effects](#)
- [Off-line Single-Stage SEPIC-Buck Converter for Dimmable LED Lighting with Reduced Storage Capacitor](#)
- [Reduction of power losses in measurement subsystem for tapped-inductor based LED driver](#)

12:00, Lecture, LS2g: Topic 12: Advanced Drive Control and Sensorless Techniques

- [A Torque Ripple Reduction Method by Current Sensor Offset Error Compensation](#)
- [Carrier signal based sensorless control of electrically excited synchronous machines at standstill and low speed using the rotor winding as a receiver](#)
- [Effects of short-time power outages and open phase failures on IPMSM sensorless rotor position estimation](#)
- [Innovative Space Vector PWM control strategy for H-Bridge meeting specific Electric Vehicle drive constraints](#)

14:50, Dialogue, DS1a: Topic 2: Passive components, system integration and packaging

- [A Methodology for Studying Aluminum Electrolytic Capacitors Wear-out in Automotive Cases](#)
- [A review on real time physical measurement techniques and their attempt to predict wear out status of IGBT](#)
- [Analysis of the plastic deformation in aluminium metallizations of Al<sub>2</sub>O<sub>3</sub> - based DAB substrates](#)
- [Automatic Design Optimisation for Power Electronics Modules Based on Rapid Dynamic Thermal Analysis](#)
- [Determination of the thermal and electrical contact resistance of press pack housings](#)
- [Dynamically adapting equivalent circuit model describing the EMI behaviour of magnetic components](#)
- [Evaluation of the submodel technique for FEM simulations of power electronic housings under power cycling conditions](#)
- [High Frequency Modeling of the Winding Wires of AC Machines](#)
- [High Temperature, High Frequency Micro-Inductors for Low Power DC-DC Converters](#)
- [Improved test bench for active ageing of power modules reproducing constraints close to automotive driving conditions](#)
- [Integrated Coreless Transformer for High Temperatures Design and Evaluation](#)
- [Integrated hybrid EMI filter: Study and Realization of the Active Part](#)
- [Interconnection technology for new wide band gap semiconductors](#)
- [Laminated Magnetic Materials Losses Analysis under Non-Sinusoidal Flux Waveforms in Power Electronics Systems](#)
- [Limitation of DC-side Stray Inductance by Considering Over Voltage and Short-circuit Current](#)
- [Loss Measurement of Magnetic Components under real Application Conditions](#)
- [Low-profile small-size ferrite cores for powerSiP integrated inductors](#)
- [Methodology for Identifying Wire Bond Process Quality Variation Using Ultrasonic Current Frequency Spectrum](#)
- [Novel Copper Metallization on Silicon Carbide electronic Devices enabling increased Packaging Lifetime and higher Junction-Temperatures](#)
- [Optimization of the passive thermal control system of a lithium-ion battery with heat pipes embedded in an aluminum plate](#)
- [Power cycling ageing tests at 200°C of SiC assemblies for high temperature electronics](#)
- [Processing and characterization of a 100 % low-temperature Ag-sintered three-dimensional structure](#)
- [Robustness Requirements on Semiconductors for High Power Applications](#)
- [Temperature Control for Reduced Thermal Cycling of Power Devices](#)
- [The Copper Losses of Litz-Wire Windings Due to an Air Gap](#)

14:50, Dialogue, DS1b: Topic 5: Hard Switching Converters and Control

# Open-circuit Fault Detection and Isolation for Modular Multilevel Converter Based on Sliding Mode Observer

Shuai Shao, Patrick W. Wheeler, Jon C. Clare, Alan J. Watson  
University of Nottingham

Department of Electrical and Electronic Engineering, University Park NG7 2RD. Nottingham, UK.

Phone: +44 (0) 115 846 8840

Fax: +44 (0) 115 951 5616

Email: eexss21@nottingham.ac.uk

## Keywords

<<Fault detection and isolation>>, <<modular multilevel converter>>, <<sliding mode observer>>, <<switching model>>, <<assumption>>.

## Abstract

This paper presents a fault detection and isolation (FDI) method for a Modular Multilevel Converter (MMC). This method can locate an open-circuit faulty device accurately and quickly. Based on a sliding mode observer (SMO) and a switching model of a half bridge, the approach is to assume the location of the fault, modify the observer equation and then compare the measured and observed states to verify, or otherwise, the assumption for possible fault locations. This technique requires no additional measurement elements and can easily be implemented in a microcontroller. The operation and robustness of the proposed method are confirmed using simulation results.

## Introduction

After being proposed in 2001 by Marquardt [1], the modular multilevel converter (MMC) has gained more and more attention. Besides the normal features of multilevel converters such as a modular structure, higher voltage capability, reduced voltage derivatives ( $dv/dt$ ) and high quality output voltage [2], the MMC does not require a multipulse transformer as its modular cells are fed by floating capacitors [3].

Fault detection and isolation (FDI) deals with monitoring a system, detecting anomalous situations (fault detection) and addressing their causes (fault isolation) [4, 5]. FDI can be implemented using hardware redundancy or analytical (software) redundancy. Hardware redundancy employs additional sensors, or redundant components in parallel with the process components, and an indication of the occurrence of a fault can be obtained if the behaviours of the process components are different from the redundant ones, or if the additional sensors detect abnormal signals [4, 6]. Analytical redundancy indicates a fault based on the discrepancy between the measured outputs and their estimations obtained through mathematical calculations. These mathematical approaches include the model-based approach and signal processing technique. The performance of an FDI scheme can be assessed using criteria such as [4]: (a) speed of detection/isolation, (b) sensitivity to incipient faults, (c) fault alarm rate, (d) missed fault detections, (e) incorrect fault isolation.

FDI is an important issue for an MMC. Although the MMC can tolerate an open-circuit fault for a number of cycles, the output voltage and current are distorted, moreover, the capacitor voltages of faulty arm will keep increasing, leading possibly to further destruction on other switches and capacitors (or the need to shut-down). Therefore it is vital to locate the open-circuit fault after its occurrence and take measures to reconfigure the circuit.

Given the large numbers of identical cells (half-bridges) and symmetrical structure of the converter, the process of addressing an open-circuit fault in an MMC is challenging if significant extra cost is to be avoided. Hardware redundancy can be used to detect faults by adding additional sensors to each semiconductor switching device [7], to each cell [8], or employing a gate drive module capable of detecting faults and providing feedback [9]. These additional sensors and signals increase both the cost and implementation complexity.

There are a number of analytical FDI methods available for voltage source converters (VSCs) [10, 11]. For a two-level VSC, an open-circuit fault can be located by detecting the current trajectory employing

Park's Vector [12] or by comparing the actual AC voltage with its reference [13]. These methods are however not suitable for an MMC, because there is not enough information to locate the fault.

In [14] the high frequency harmonics of the output voltage are used to locate the faulty cell of a cascaded H-bridge (CHB). Potentially this technique can also be employed for an MMC. The technique analyses the magnitude of the switching frequency component ( $v_s$ ) and the faulty cell can be located according to the angle of  $v_s$ . Nonetheless, the faulty device cannot be located and it is easy to misdiagnose during transient operation [14].

Artificial intelligence (AI)-based techniques can also be applied to fault diagnosis of an MMC or to other multilevel converters with the advantage of not requiring models of the converters. Fault detection using a neural network (NN) approach for a CHB was proposed in [11]. The major drawback of these techniques is accuracy, only 76% in some cases. Moreover, it can take a long time to train the algorithms for the circuit topology and all the fault scenarios.

This paper proposes a sliding mode observer (SMO) based fault detection method for an MMC (Fig. 1). The method uses the inputs which are already available as measurement inputs to the control system. Using this method not only the faulty cell, but also the faulty switching device can be located. Due to the SMO robustness [15, 16, 17], this method can discriminate an open-circuit fault (for whatever reason, including gate drive failure) from the disturbance caused by measurement noise and parameter uncertainty. The fault condition of a semiconductor switching device appearing as an open circuit will be investigated in this paper.

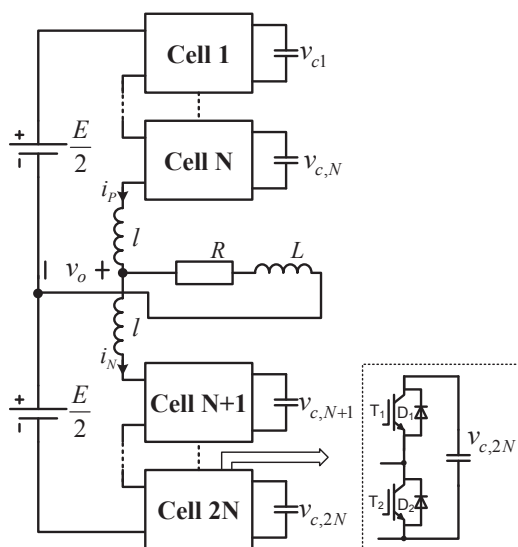


Figure 1: A single phase MMC

## Model of A Half-bridge

This section presents the switching model of a half-bridge both in normal and faulty conditions, as these models are vital for the FDI of an MMC.

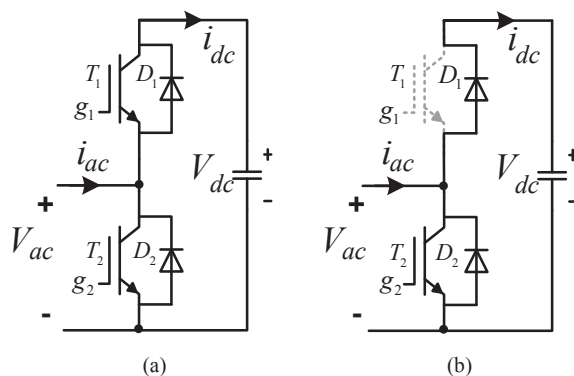


Figure 2: Switching model of half-bridge. (a) Normal condition. (b) Fault condition (an open-circuit fault at  $T_1$ ).



Fig. 2 shows the submodule of an MMC, where  $g_1$  and  $g_2$  are the gate signals for switches, and are complementary. When the gate signal is 1, the corresponding switch turns on; when it is 0, the corresponding switch turns off.

### Normal (fault-free) condition

As shown in Fig. 2(a), when  $g_1 = 1, g_2 = 0$ ,  $T_1$  is on and  $T_2$  is off, thus  $V_{ac} = V_{dc}, i_{dc} = i_{ac}$ ; alternatively, when  $g_1 = 0, g_2 = 1$ ,  $V_{ac} = 0, i_{dc} = 0$ . Therefore, the relationship between the AC-side and DC-side voltages and currents can be calculated as

$$\begin{cases} V_{ac} = S \cdot V_{dc} \\ i_{dc} = S \cdot i_{ac} \end{cases}, \quad (1)$$

where  $S$  is the switching state given by Table I.

Table I: Switching state  $S$  in normal condition

S	Driving signals
1	$g_1 = 1, g_2 = 0$
0	$g_1 = 0, g_2 = 1$

Table II: Switching state  $S$  in fault condition

Location of the fault	Condition	Switching State	
		Normal	Fault
$T_1$	$g_1 = 1, i_{ac} < 0$	1	$S_F = 0$
	Other conditions	S	$S_F = S$
$T_2$	$g_2 = 1, i_{ac} > 0$	0	$S_F = 1$
	Other conditions	S	$S_F = S$

### Fault condition

In the fault condition (one open-circuit fault of the switch), the switching models can still be described as shown in (1), but the switching states  $S$  in (1) have to be modified. Consider the half-bridge with an open circuit fault at  $T_1$ , as shown in Fig. 2(b). When  $g_1 = 1, i_{ac} < 0$ ,  $i_{ac}$  is forced to go through  $D_2$  instead of  $T_1$  because of the open-circuit fault. Thus, the switching state  $S$  should be changed from 1 to 0. For all other conditions, the half-bridge operates as normal. When the open-circuit fault occurs on  $T_2$ , the switching state can be modified in a similar way. Table II presents the modifications of the switching states for a faulty half-bridge.

The analysis assumes ideal devices and instantaneous commutation. The fault detection method is however robust against non-ideal device characteristics. This is verified in the all of the simulation results where generous values of 5V and 1 $\mu$ s are included for the device voltage drop and dead-time delay respectively.

### Sliding Mode Observer of an MMC

An observer is a contrivance designed from a real system, generally in the same mathematical form as the original system, so as to estimate its internal state [15][18]. An SMO uses a high feedback gain in the observer vector (normally in the form of a high frequency switching function, for example the saturation function of an observed-measured error, as (3) and (4) present) to force the observed output to converge to a measured output [15][17]. The SMO offers desirable features such as robustness to parameter uncertainty and insensitivity to measurement noise [15, 16, 17]. With a simple realisation, the SMO can be implemented in a field-programmable gate array (FPGA) [18][19].

A sliding mode observer for a second-order system using the equivalent control method will be developed first[20, 21], then the SMO equations for an eight-cell MMC and the corresponding simulated results will be given.

Consider a second-order system which is observable,

$$\begin{bmatrix} \dot{x}_1 \\ \dot{x}_2 \end{bmatrix} = \begin{bmatrix} a_{11} & a_{12} \\ a_{21} & a_{22} \end{bmatrix} \begin{bmatrix} x_1 \\ x_2 \end{bmatrix} + \begin{bmatrix} b_1 \\ b_2 \end{bmatrix} u, \quad (2)$$

we can use the high-gain feedback  $L \cdot \text{sat}(x - \hat{x})$  to obtain the observed states

$$\begin{cases} \dot{\hat{x}}_1 = a_{11}\hat{x}_1 + a_{12}\hat{x}_2 + b_1u + L_1\text{sat}(x_1 - \hat{x}_1) \\ \dot{\hat{x}}_2 = a_{21}\hat{x}_1 + a_{22}\hat{x}_2 + b_2u + L_2\text{sat}(x_2 - \hat{x}_2), \end{cases} \quad (3)$$









IMMIGRATION OFFICER  
 (60132) \*  
 - 2 NOV 2012 \*  
 BIRMINGHAM

中国边检 CHINA  
 浦东(入)  
 2014-02-12  
 中国边检 CHINA  
 浦东(入)  
 2015-04-02

IMMIGRATION OFFICER  
 (6167) \*  
 - 6 AUG 2013 \*  
 MANCHESTER (1)

中国边检 CHINA  
 浦东  
 2014-03-19

IMMIGRATION OFFICER  
 (6019) \*  
 - 15 SEP 2013 \*  
 LILLE

G50216582

IMMIGRATION OFFICER  
 (6012) \*  
 - 3 MAR 2014 \*  
 BIRMINGHAM

中国边检 CHINA  
 浦东(出)  
 2015-04-12

DEPARTMENT OF HOMELAND SECURITY  
 U.S. CUSTOMS AND BORDER PROTECTION  
 ADMITTED  
 SEP 13 2014  
 12 AUG 2014  
 3264

IMMIGRATION OFFICER  
 (003)  
 24 SEP 2014  
 SHANNON AIRPORT

TRANS. T GULY FOR  
 (16)

14 AUG 2015




姓名 邵 帅

性别 男 民族 汉

出生 1987 年 12 月 11 日

住址 杭州市西湖区余杭塘路  
3 8 8 号



公民身份号码 430981198712114676



中华人民共和国  
居民 身 份 证

签发机关 杭州市公安局西湖分局

有效期限 2006.12.06-2016.12.06

依据《浙江省人民政府关于引进海外高层次留学人才的意见》(浙政发[2001]28号), 特发此证。



浙江省人力资源和社会保障厅



发证机关: 浙江省人力资源和社会保障厅  
Issued by

编号: 002346  
Number

发证日期: 2016 年 03 月 01 日  
Conferral Date

姓名 邵帅  
Full Name

性别 男  
Sex

出生年月 1987 年 12 月 11 日  
Date of Birth YY MM DD

国籍 中国  
Nationality

身份证(护照)号码 430981198712114676  
ID(passport) Number

聘用单位 浙江大学电气学院  
Employer

居住地址 杭州求是村留博楼 303 室  
Address

有效期至 2019 年 02 月 28 日



# 聘用合同

甲方(用人单位)名称: 浙江工业大学  
法定代表人(或主要负责人): \_\_\_\_\_  
注册地址: \_\_\_\_\_  
经营地址: \_\_\_\_\_

乙方(劳动者)姓名: 邵帅  
性别: 男 居民身份证号码: 430981198712114676  
居住地联系电话: \_\_\_\_\_ 手机号码: 15868126530  
现居住地址: 杭州市西湖区求是村留博楼B03 邮编: 310613  
户口所在地: 杭州市西湖区浙大路38号 邮编: 310027

根据相关法律、法规的规定,经甲乙双方平等自愿、协商一致,共同签订并履行本合同所列条款。

## 第一条 聘用合同类型及期限

一、本聘用合同类型及期限按下列第 1 项确定。

1、固定期限:自 2015 年 11 月 26 日起至 2018 年 12 月 31 日止。

2、无固定期限:自 \_\_\_\_\_ 年 \_\_\_\_\_ 月 \_\_\_\_\_ 日起至法定的解除或终止合同的条件出现时止。

3、以完成一定工作任务为期限:自 \_\_\_\_\_ 年 \_\_\_\_\_ 月 \_\_\_\_\_ 日起至 \_\_\_\_\_ 终止。

二、本合同约定试用期的,试用期自 \_\_\_\_\_ 年 \_\_\_\_\_ 月 \_\_\_\_\_ 日起至 \_\_\_\_\_ 年 \_\_\_\_\_ 月 \_\_\_\_\_ 日止。

## 第二条 工作内容和工作地点

一、乙方同意根据甲方生产(工作)需要,从事 \_\_\_\_\_ 工作。甲乙双方

可另行约定岗位具体职责和要求。乙方应按照甲方制定的规章制度和岗位职责要求认真履行义务,按时、按质、按量完成工作任务。未经甲方书面许可不得同时与其他用人单位建立劳动聘用关系。

二、乙方的工作地点为: \_\_\_\_\_

三、对变更工作岗位事宜，双方作如下约定：

1、甲方可以根据工作需要、岗位职责、岗位聘任制度、乙方工作能力等因素对乙方实行综合考核，并视乙方工作岗位考核情况作出相应调整。

---

---

---

---

四、甲乙双方对工作内容和工作地点的其他约定：

---

---

### 第三条 工作时间和休息休假

一、乙方在合同期内的工时制度、休息休假制度等按照甲方依法制定的规章制度和国家、本省、市有关法律法规规定执行。

二、甲方根据工作需要，安排乙方加班、加点，必须遵守有关法律法规规定。甲方依法保证乙方的休息休假权利。

### 第四条 工作报酬

一、乙方试用期间的月基本工资为\_\_\_\_\_元。

二、试用期满后，乙方在法定工作时间内提供正常劳动的月基本工资为\_\_\_\_\_元或根据甲方确定的薪酬制度确定为\_\_\_\_\_。

\_\_\_\_\_。乙方岗位职级依照本合同第二条第三款发生变更的，工作报酬需做相应调整。

乙方工资的增减，奖金、津贴、补贴、加班加点工资的发放，以及特殊情况下的工资支付等，均按相关法律法规及甲方依法制定的规章制度执行。甲方支付给乙方的工资不得低于当地最低工资标准。加班工资以上述基本工资为基数计算，如基本工资低于最低工资标准，以最低工资标准为基数计算。

三、甲方的工资发放日为每月\_\_\_\_\_。甲方应当以货币形式按月支付工资，不得无故拖欠。

四、乙方在享受法定节假日以及依法参加社会活动期间，甲方应当依法支付工资。

五、甲乙双方对工作报酬的其他约定：\_\_\_\_\_

---

---

### 第五条 社会保险

甲乙双方必须依法参加社会保险，按月缴纳社会保险费。乙方缴纳部分，由甲方在乙方工资中代为扣缴。



## 第六条 劳动保护、劳动条件和职业危害防护

甲乙双方都必须严格执行国家有关安全生产、劳动保护、职业卫生等规定。有职业危害的工种应在合同约定中告知，甲方应为乙方的生产工作提供符合规定的劳动保护设施、劳动防护用品及其他劳动保护条件。乙方应严格遵守各项安全操作规程。甲方必须自觉执行国家有关女职工劳动保护和未成年工特殊保护规定。

## 第七条 规章制度

- 一、甲方依法制定单位规章制度，并已通过有效方式及时告知乙方。
- 二、乙方服从甲方工作管理，并严格遵守甲方依法制定的规章制度。

## 第八条 聘用合同变更、解除和终止

一、甲乙双方变更、解除、终止聘用合同依照相关法律法规规定执行。甲乙双方就聘用合同变更、解除另有约定的，可在本合同书第九条中约定。

二、甲乙双方解除或者终止聘用合同后，甲方应为乙方出具解除或者终止聘用合同的证明。乙方应按甲方规定，及时办理工作交接等有关手续。甲方应当支付经济补偿的，在乙方办结工作交接等有关手续时支付。若乙方迟延交接或者交接手续不齐全，应赔偿由此造成甲方的相关损失。

## 第九条 双方需要约定的其他事项

经协商一致，甲乙双方约定以下内容：

---

---

---

---

---

---

---

---

---

---

---

---

## 第十条 聘用合同的无效

甲方有权了解乙方与聘用合同直接相关的基本情况，包括但不限于劳动者的身份证明、学历、履历、资格或任职证书（明）以及以前劳动关系解除或终止证明等。乙方应当如实说明，并保证出具的证明或文件等资料真实、合法、有效。乙方承诺与原用人单位之间不存在任何违反竞业限制或侵犯商业秘密等事项。如有欺诈、隐瞒或重大遗漏，使甲方在违背真实意志的情况下订立或变更聘用合同的，则聘用合同无效或者部分无效。

## 第十一条 解除、终止和违反聘用合同的责任

一、甲、乙任何一方违反本合同，给对方造成损失的，应当赔偿损失。

二、乙方有下列情形之一的，应当依法赔偿甲方损失：

1、因乙方隐瞒与其他用人单位尚未解除或者终止劳动合同事实的，给其他用人单位造成损失的，最终导致甲方承担连带赔偿责任，乙方应当赔偿由此造成甲方的损失。

2、乙方违法解除聘用合同、违反保密义务或者竞业限制约定，给甲方造成损失的，应当承担赔偿责任。

3、乙方对外违法招用劳动者，导致甲方承担连带责任的，乙方应当赔偿由此造成甲方的损失。

4、因乙方过错致使本合同被确认无效，给甲方造成损害的，乙方应当承担赔偿责任。

5、由甲方出资对乙方进行的专业技术培训，乙方违反服务期约定的，应当向甲方支付违约金，违约金数额为服务期尚未履行部分所应分摊的培训费用。详见《专业技术培训协议》。

6、竞业限制违约及赔偿详见保密协议或竞业限制条款。

7、上述赔偿损失的范围包括但不限于：生产经营损失；招聘费用；培训费用；第三人索赔；行政处罚等。

8、如果乙方欠付甲方任何款项或应承担依照法律和本合同约定的赔偿责任，甲方有权在不违反法律法规之前提下，从乙方的奖金或工资中做相应的扣除，不足部分，甲方有权向乙方追偿。

## 第十二条 争议处理及其他

一、甲乙双方因履行聘用合同发生争议，应协商解决，协商不成或不愿协商的，可以向仲裁机构申请仲裁。对仲裁裁决不服的，可以向人民法院起诉。

二、乙方确认本合同所列现居住地址为本合同相关文件、文书的送达和通知地址。如该地址变更，乙方应及时书面告知甲方，甲方将需送达的资料邮寄至该地址，即视为送达。

三、本合同未尽事项，按国家有关法律法规执行。

四、本合同条款如与今后国家颁布的法律法规相抵触时，按国家新的法律法规执行。

五、本合同依法订立，双方签字盖章后生效，双方必须严格履行。

六、本合同一式\_\_\_\_份，甲乙双方各执一份。

甲方（盖章）：

乙方（签字）：

甲方法定代表人（主要负责人）

或委托代理人（签字或盖章）：

签约日期：2015年11月26日

签约日期：2015年11月26日



附件：

## 浙江大学教学科研人员聘用合同补充协议

浙江大学委托 电气学院 单位（甲方）与 邵帅（乙方）就聘用乙方到甲方工作事宜，签订以下补充协议，作为《聘用合同书》的附件：

一、根据甲方的工作需要和岗位设置，乙方应聘到甲方 教学科研岗 岗位上工作。甲方经过对乙方的考核，同意聘用乙方到甲方工作。

二、聘用期限详见《聘用合同书》（本聘期应与校内聘岗期限一致）。

三、在聘用期间，甲方按有关规定向乙方提供工资；养老、医疗等社会保险按国家有关政策规定执行。住房实行货币化安置。科研启动经费的发放、教师岗位聘任、专业技术职务晋升等根据学校有关规定执行。乙方应制定聘期内科研启动经费总预算计划和年度预算计划，并严格按计划使用；对未能按预算计划使用的结余经费及聘期末结余经费额度，学校有权按相关规定收回。

四、在聘用期间，乙方应遵守国家法律、法规和学校的规章制度；认真完成聘期教学科研工作目标（任务书另附），甲方按任务书所确定的工作目标对乙方进行期满考核和评估。对违反校纪校规或经考核不能胜任本职工作的，甲方有权按学校相关规定进行处理直至解除聘用关系。

五、聘用期满考核业绩优秀，经双方商定需继续聘用的可续签协议；如一方决定不再续聘的，应于协议期满前一个月以书面形式向对方提出。解除或终止聘用合同后尚未落实新工作单位的，应将个人档案委托当地人才中心等部门管理。

六、乙方在聘用期间如享受过甲方提供的各类专项培训的，在聘用期间如向甲方提出自费出国（不含经批准的短期探亲、旅游等）、解除合同等，视作违约行为。除法律、法规及聘用合同与本协议规定的内容以外，甲、乙双方不得以其它理由单方面解除合同，如有违约行为，违约方需一次性支付违约金，违约金额为甲方提供的各类专项培训费用总额。同时根据违约年限，按比例归还科研启动经费和各项配套经费。

七、乙方确认聘用合同所列联系地址及 Email 为聘用期间相关文件、文书的送达和通知地址及邮箱。甲方将需送达的资料邮寄或发送至该地址，即视为送达。如该地址变更，乙方应及时书面告知甲方。

八、本协议自甲、乙双方签字盖章后生效。《聘用合同书》与本协议各一式三份（甲、乙双方和学校人事处各执壹份），具有同等效力。

甲方（盖章）

甲方代表签字：

2015年11月26日

乙方签字：邵帅

2015年11月26日





浙大人证字第0015185 号

发证日期 20 15 年 11 月 30 日

姓名 邵帅

性别 男

民族 汉族

出生年月 1987. 12. 11

籍贯 湖南益阳

职别 教师

部门 电气学院



# THE UNIVERSITY OF NOTTINGHAM

It is hereby certified that after having satisfied all the  
conditions prescribed by the University

**SHUAI SHAO**

was on the

sixteenth day of July, 2015

duly admitted to the degree of

Doctor of Philosophy



*Vice-Chancellor*

*Registrar*





教育部留学服务中心

Chinese Service Center for Scholarly Exchange

## 国外学历学位认证书

教留服认英[2016]02340号

邵帅，男，中国国籍，1987年12月11日生于湖南省。

邵帅2011年11月起在英国诺丁汉大学（University of Nottingham）从事电气与电子工程专业研究，论文通过，于2015年7月获得该校颁发的哲学博士学位证书。

经核查，诺丁汉大学系英国正规高等学校。邵帅所获博士学位证书表明其具有相应的学历。

